Fourth-order multiple-relaxation-time lattice Boltzmann model and equivalent finite-difference scheme for one-dimensional convection-diffusion equations

Ying Chen [1], Zhenhua Chai [1,2,3,*] and Baochang Shi [1,3]

[1] *School of Mathematics and Statistics, Huazhong University of Science and Technology, Wuhan 430074, China*

[2] *Institute of Interdisciplinary Research for Mathematics and Applied Science, Huazhong University of Science and Technology, Wuhan 430074, China*

[3] *Hubei Key Laboratory of Engineering Modeling and Scientific Computing, Huazhong University of Science and Technology, Wuhan 430074, China*

(Received 14 November 2022; accepted 12 April 2023; published 12 May 2023)

In this paper, we first develop a fourth-order multiple-relaxation-time lattice Boltzmann (MRT-LB) model for the one-dimensional convection-diffusion equation (CDE) with the constant velocity and diffusion coefficient, where the D1Q3 (three discrete velocities in one-dimensional space) lattice structure is used. We also perform the Chapman-Enskog analysis to recover the CDE from the MRT-LB model. Then an explicit four-level finite-difference (FLFD) scheme is derived from the developed MRT-LB model for the CDE. Through the Taylor expansion, the truncation error of the FLFD scheme is obtained, and at the diffusive scaling, the FLFD scheme can achieve the fourth-order accuracy in space. After that, we present a stability analysis and derive the same stability condition for the MRT-LB model and FLFD scheme. Finally, we perform some numerical experiments to test the MRT-LB model and FLFD scheme, and the numerical results show that they have a fourth-order convergence rate in space, which is consistent with our theoretical analysis.

DOI: 10.1103/PhysRevE.107.055305

I. INTRODUCTION

Lattice Boltzmann (LB) method, as a mesoscopic numerical approach originated from the lattice gas automata or developed from the simplified kinetic model, has been an effectively computational tool in the study of complex flow problems [1–6]. On the other hand, the LB method has also been used to solve some different kinds of partial difference equations (PDEs) for complex physical systems, for example, the diffusion equations [7–9], convection-diffusion equations [10–22], Possion equation [23–25], Burgers equation [26], and some other complex equations [27–30].

The evolution process of the LB method can be split into the collision and propagation steps, and they are a system of explicit two-level finite-difference equations of the distribution functions in different directions. Based on the collision term in the LB method, the models can be divided into three main categories, the lattice Bhatnagar-Gross-Krook (BGK) or single-relaxation-time LB (SRT-LB) model [31], two-relaxation-time LB (TRT-LB) model [12], and multiple-relaxation-time LB (MRT-LB) model [32]. The SRT-LB model is most efficient, while it also has some limitations. The first is that it suffers from the stability problem when the relaxation parameter is close to its limit value [16,33]. The second is that the SRT-LB model does not have sufficient relaxation parameters to describe the anisotropic diffusion process, which also makes it more difficult in solving the anisotropic CDEs [4,34]. The TRT-LB model has a free relaxation parameter that can be used to improve the stability and/or accuracy by selecting the so-called magic parameter Λ^{eo} properly [5]. We note that the SRT-LB and TRT-LB models are two special cases of the MRT-LB model [32], and compared to the SRT-LB and TRT-LB models, the MRT-LB model is more general and could be more stable through adjusting additional free relaxation parameters [34–37]. For these reasons, we will focus on the MRT-LB model in this work.

It is known that there are some asymptotic analysis methods, including the Chapman-Enskog analysis [38], the Maxwell iteration [39,40], the direct Taylor expansion [41–43], and the equivalent equations [44,45] that have been used to study the consistency of LB models, but they are not suitable to construct a rigorous notion of consistency and perform an accuracy analysis with respect to the target PDEs. This is mainly caused by the fact that the relation between the LB model and the macroscopic PDE based numerical scheme (the macroscopic or equivalent numerical scheme hereafter) is unclear.

To fill the gap, some researchers conducted the theoretical analysis on the equivalent finite-difference schemes of several particular LB models for the macroscopic governing equations on the conserved variables (or conservative moments). For instance, Junk [46] and Inamuro [47] found that the SRT-LB model is equivalent to a two-level difference scheme when the relaxation parameter is equal to unity, and at the diffusive scaling, a second-order convergence rate in space can be achieved for the incompressible Naiver-Stokes equations [46]. Ancona [48] presented an LB model with D1Q2 lattice structure for one-dimensional CDEs and found

*Corresponding author: hustczh@hust.edu.cn

that this model can be written as the three-level second-order DuFort-Frankel scheme [49]. Li *et al.* [26] considered the SRT-LB model for one-dimensional Burgers equation where the D1Q2 lattice structure is adopted and derived a three-level second-order finite-difference scheme. Dellacherie [50] carried out an analysis on the SRT-LB model with D1Q2 lattice structure for one-dimensional CDEs and demonstrated that this LB model is equivalent to an explicit two-level finite-difference scheme. Cui *et al.* [36] found that the MRT-LB model is equivalent to a macroscopic second-order finite-difference scheme for one-dimensional steady CDE. Bellotti *et al.* [51,52] presented a detailed study on the relation between the MRT-LB model and the macroscopic numerical scheme and further demonstrated that any LB models can be rewritten as the second-order finite-difference schemes. However, it should be noted that the general finite-difference scheme shown in the previous work [51] and other schemes mentioned above are all of second-order accuracy, which is consistent with the results based on some asymptotic analysis methods for the LB models [32]. d'Humière and Ginzburg [53] conducted a theoretical analysis on the TRT-LB model with recurrence equations and illustrated that when the magic parameter $\Lambda^{eo} = 1/4$ the TRT-LB model would reduce to a macroscopic three-level finite difference scheme with a second-order accuracy in space. Subsequently, Ginzburg [54] further found that for the TRT-LB model with $\Lambda^{eo} = 1/6$ and $\Lambda^{\mathrm{BGK}} = 1/12$, the fourth-order truncation error for diffusion equations can be removed, and the third-order truncation error for CDEs can be removed with $\Lambda^{eo} = \Lambda^{\mathrm{BGK}} = 1/12$. Recently, through adjusting the weight coefficients and relaxation parameters properly, Lin [8] developed a macroscopic four-level sixth-order finite-difference scheme from the MRT-LB model for the one-dimensional diffusion equation, where the D1Q3 lattice structure is used. Particularly, for the SRT-LB model, i.e., all relaxation parameters in the MRT-LB model are equal to each other, this sixth-order finite-difference scheme would reduce to a fourth-order one, which is same as that reported in Ref. [9]. Straka *et al.* [10] considered a cascaded SRT-LB model, and obtained an equivalent higher-order finite-difference scheme for one-dimensional advection-diffusion equation. However, it is still unclear whether we can give a fourth-order LB model and the corresponding macroscopic finite-difference scheme for CDE. In this work, we will first develop a high-order MRT-LB model for the one-dimensional CDE with the constant velocity and diffusion coefficient, and show that through the Chapman-Enskog analysis, the CDE can be recovered correctly from this MRT-LB model. We then also consider the equivalent finite-difference scheme of the MRT-LB model and find that at the diffusive scaling both the MRT-LB model and equivalent finite-difference scheme can achieve a fourth-order convergence rate in space.

This paper is organized as follows. In Sec. II, we present an MRT-LB model with the D1Q3 lattice structure for the one-dimensional CDE where a modified equilibrium function is adopted. In Sec. III, through a theoretical analysis, we obtain an explicit four-level finite-difference (FLFD) scheme from the MRT-LB model. In Sec. IV, the accuracy and stability analysis of the MRT-LB model and FLFD scheme are conducted through the Taylor expansion and Von Neumann stability analysis method. In Sec. V, we carry out some numerical experiments and show that both the MRT-LB model and FLFD scheme can achieve a fourth-order convergence rate in space, which is consistent with our theoretical analysis. Finally, we give some conclusions in Sec. VI.

II. FOURTH-ORDER MULTIPLE-RELAXATION-TIME LATTICE BOLTZMANN MODEL FOR ONE-DIMENSIONAL CONVECTION-DIFFUSION EQUATIONS

In this section, we first develop an MRT-LB model for the one-dimensional CDE with the constant velocity and diffusion coefficient and then perform the Chapman-Enskog analysis to derive the CDE from the present MRT-LB model.

A. Spatial and temporial discretization

In the LB method, the space is discretized by the lattice $\mathcal{L} := \Delta x\mathbb{Z}$ with the lattice spacing $\Delta x > 0$, the time is uniformly discretized with $t_n = n\Delta t$, and Δt is the time step. For the sake of brevity and to simplify the following analysis, the so-called lattice velocity defined by $c := \Delta x/\Delta t$ is also introduced.

B. Multiple-relaxation-time lattice Boltzmann model

From the mathematical point of view, the one-dimensional CDE with the constant convection velocity u and diffusion coefficient κ can be written as

$$\frac{\partial \phi}{\partial t} + u\frac{\partial \phi}{\partial x} = \kappa \frac{\partial^2 \phi}{\partial x^2}, \tag{1}$$

where ϕ is a scalar variable dependent on the space x and time t. Here we only consider the more general MRT-LB model for its good accuracy and stability in the study of complex problems [18,19,32,55]. For the CDE (1), the evolution equation of the MRT-LB model can be rewritten as [19,36]

$$\begin{aligned} &f_i(x + c_i\Delta t, t + \Delta t) \\ &\quad = f_i(x,t) - (\boldsymbol{M}^{-1}\boldsymbol{S}\boldsymbol{M})_{i,k}\left[f_k(x,t) - f_k^{\mathrm{eq}}(x,t)\right], \end{aligned} \tag{2}$$

where $f_i(x,t)$ and $f_i^{\mathrm{eq}}(x,t)$ are the distribution function and equilibrium distribution function at position x and time t, respectively. In the D1Q3 lattice structure, the discrete velocity c_i, the transform matrix $\boldsymbol{M}$ and the diagonal relaxation matrix $\boldsymbol{S}$ can be given by

$$c_0 = 0, \quad c_1 = c, \quad c_{-1} = -c, \tag{3a}$$

$$\boldsymbol{M} = \begin{pmatrix} 1 & 1 & 1 \\ 0 & c & -c \\ -2c^2 & c^2 & c^2 \end{pmatrix}, \tag{3b}$$

$$\boldsymbol{S} = \begin{pmatrix} s_0 & 0 & 0 \\ 0 & s_1 & 0 \\ 0 & 0 & s_2 \end{pmatrix}, \tag{3c}$$

where the diagonal element s_i of the relaxation matrix $\boldsymbol{S}$ is the relaxation parameter corresponding to ith moment of the distribution functions. To ensure the physical transport coefficient (e.g., diffusion coefficient) to be positive, s_i should be located in the range (0,2).

In the evolution equation (2), the equilibrium distribution is designed as

$$f_i^{\rm eq} = w_i\phi\left[1 + \frac{c_i u}{c_s^2} + \eta\frac{u^2\left(c_i^2 - c_s^2\right)}{2c_s^4}\right], \tag{4}$$

where w_i is the weight coefficient and η is a parameter to be determined below.

To derive correct CDE (1), the equilibrium distribution function should satisfy the following conditions:

$$\sum_i f_i^{\rm eq} = \phi, \tag{5a}$$

$$\sum_i f_i^{\rm eq} c_i = \phi u, \tag{5b}$$

$$\sum_i f_i^{\rm eq} c_i c_i = \left(c_s^2 + u^2\right)\phi. \tag{5c}$$

From Eq. (5), one can obtain

$$c_s^2 = (1 - w_0)c^2, \tag{6a}$$

$$\eta = \frac{2(1 - w_0)}{w_0}, \tag{6b}$$

$$w_1 = w_{-1} = \frac{1 - w_0}{2}, \tag{6c}$$

where the weight coefficient w_0 ($0 < w_0 < 1$) can be considered as a free parameter. In addition, the macroscopic variable $\phi(x, t)$ (or the conservative moment) is calculated by

$$\phi(x, t) = \sum_i f_i(x, t). \tag{7}$$

C. The Chapman-Enskog analysis

In this part, we will present the Chapman-Enskog analysis [38] to derive Eq. (1) from above MRT-LB model. In the Chapman-Enskog analysis, the distribution function, the time and space derivatives can be expressed as [33]

$$f_i = f_i^{(0)} + \epsilon^1 f_i^{(1)} + \epsilon^2 f_i^{(2)} + \cdots, \quad \partial_t = \epsilon^1\partial_{t_1} + \epsilon^2\partial_{t_2},$$
$$\partial_x = \epsilon^1\partial_{x_1}, \tag{8}$$

where ϵ is a small parameter. Substituting Eq. (8) into Eq. (2) and using Taylor expansion, we can obtain zero-, first-, and second-order equations in ϵ,

$$\epsilon^0 : f_i^{(0)} = f_i^{\rm eq}, \tag{9a}$$

$$\epsilon^1 : D_{1,i} f_i^{(0)} = -\frac{1}{\Delta t}(\boldsymbol{M}^{-1}\boldsymbol{S}\boldsymbol{M})_{i,k} f_k^{(1)}, \tag{9b}$$

$$\epsilon^2 : \partial_{t_2} f_i^{(0)} + D_{1,i} f_i^{(1)} + \frac{\Delta t}{2} D_{1,i}^2 f_i^{(0)} = -\frac{1}{\Delta t}(\boldsymbol{M}^{-1}\boldsymbol{S}\boldsymbol{M})_{i,k} f_k^{(2)}, \tag{9c}$$

where $D_{1,i} = \partial_{t_1} + c_i\partial_{x_1}$.

If we multiply $D_{1,i}$ on both sides of Eq. (9b), and substitute it into Eq. (9c), then we can rewrite Eq. (9c) as

$$\epsilon^2 : \partial_{t_2} f_i^{(0)} + D_{1,i}\left(\boldsymbol{I} - \frac{\boldsymbol{M}^{-1}\boldsymbol{S}\boldsymbol{M}}{2}\right)_{i,k} f_k^{(1)} = -\frac{1}{\Delta t}(\boldsymbol{M}^{-1}\boldsymbol{S}\boldsymbol{M})_{i,k} f_k^{(2)}. \tag{10}$$

Taking the zeroth and first moments of Eq. (9b) and the zeroth moment of Eq. (9c), one can obtain the following equations:

$$\partial_{t_1}\phi + \partial_{x_1}(\phi u) = 0, \tag{11a}$$

$$-u^2\partial_{x_1}\phi + \left(c_s^2 + u^2\right)\partial_{x_1}\phi = -\frac{1}{\Delta t}\sum_i c_i(\boldsymbol{M}^{-1}\boldsymbol{S}\boldsymbol{M})_{i,k} f_k^{(1)}, \tag{11b}$$

$$\partial_{t_2}\phi + \partial_{x_1}\sum_i c_i\left(\boldsymbol{I} - \frac{\boldsymbol{M}^{-1}\boldsymbol{S}\boldsymbol{M}}{2}\right)_{i,k} f_k^{(1)} = 0, \tag{11c}$$

where Eqs. (5) and (9a) have been used. Then substituting Eq. (11b) into Eq. (11c), we have

$$\partial_{t_2}\phi = c_s^2\left(\frac{1}{s_1} - \frac{1}{2}\right)\Delta t\,\partial_{x_1}^2\phi. \tag{12}$$

Through combining the results at t_1 and t_2 scales, i.e., Eqs. (11a) and (12), we can recover the CDE (1) with the following diffusion coefficient:

$$\kappa = c_s^2\left(\frac{1}{s_1} - \frac{1}{2}\right)\Delta t. \tag{13}$$

Finally, we would also like to point out that the numerical diffusion related to u^2 in the previous LB models [12,15] can be eliminated here such that the diffusion coefficient κ is independent on velocity u [see Eq. (13)]. This is because a modified equilibrium distribution function (4) with the parameter $\eta = 2(1 - w_0)/w_0$ is adopted in the present MRT-LB model.

III. AN EXPLICIT FOUR-LEVEL FINITE-DIFFERENCE SCHEME

In this section, we will show some details on how to derive the explicit finite-difference scheme for Eq. (1) from above MRT-LB model. It is known that any LB models can be divided into two processes: a local collision step performed on each site of the lattice and a propagation step conducted among neighboring sites of the lattice. Based on this fact, we multiply $\boldsymbol{M}$ on both sides of Eq. (2) and express the collision step in a vector form,

$$\boldsymbol{m}^\star(x, t) = (\boldsymbol{I} - \boldsymbol{S})\boldsymbol{m}(x, t) + \boldsymbol{S}\boldsymbol{m}^{\rm eq}(x, t), \ x \in \mathcal{L}, \tag{14}$$

where the postcollision state is denoted by $\star$, the relation between the postcollision distribution function $\boldsymbol{f}^\star(x, t) = (f_0^\star, f_1^\star, f_{-1}^\star)^T$ and $\boldsymbol{m}^\star$ is given by $\boldsymbol{m}^\star = \boldsymbol{M}\boldsymbol{f}^\star$.

According to the definition of shift operator $T_{\Delta x}^{c_k/c}$ $\{T_{\Delta x}^{c_k/c}[f_i(x, t)] = f_i(x - c_k\Delta t, t)\}$ [51], the propagation step can be written as

$$\boldsymbol{f}(x + \boldsymbol{c}\Delta t, t + \Delta t) = \mathbf{diag}\left(T_{\Delta x}^{c_0/c}, T_{\Delta x}^{c_{-1}/c}, T_{\Delta x}^{c_1/c}\right)\boldsymbol{f}^\star(x, t), \ x \in \mathcal{L}, \tag{15}$$

where $\boldsymbol{f}(x, t) = (f_0, f_1, f_{-1})^T$, $\boldsymbol{c} = (c_0, c_1, c_{-1})^T$. If we multiply $\boldsymbol{M}$ on both sides of Eq. (15) and with the help of Eq. (14), then one can obtain

$$\boldsymbol{m}^{n+1}(x) = \boldsymbol{P}\boldsymbol{m}^n(x) + \boldsymbol{Q}\boldsymbol{m}^{{\rm eq}|n}(x), \ x \in \mathcal{L}, \tag{16}$$

where $\boldsymbol{m}^n(x) = \boldsymbol{m}(x, t_n)$, $\boldsymbol{T} := \boldsymbol{M}\mathbf{diag}(T_{\Delta x}^{c_0/c}, T_{\Delta x}^{c_1/c}, T_{\Delta x}^{c_{-1}/c})\boldsymbol{M}^{-1}$, $\boldsymbol{P} := \boldsymbol{T}(\boldsymbol{I} - \boldsymbol{S})$, and $\boldsymbol{Q} := \boldsymbol{T}\boldsymbol{S}$.

After some algebraic manipulations, one can obtain the matrices $\boldsymbol{T}$, $\boldsymbol{P}$, and $\boldsymbol{Q}$,

$$\boldsymbol{T}=\begin{bmatrix} \frac{1}{3}\left(T_{\Delta x}^{c_{-1}/c}+T_{\Delta x}^{c_0/c}+T_{\Delta x}^{c_1/c}\right) & \frac{1}{2c}\left(T_{\Delta x}^{c_{-1}/c}-T_{\Delta x}^{c_1/c}\right) & \frac{1}{6c^2}\left(T_{\Delta x}^{c_{-1}/c}-2T_{\Delta x}^{c_0/c}+T_{\Delta x}^{c_1/c}\right) \\ \frac{c}{3}\left(T_{\Delta x}^{c_{-1}/c}-T_{\Delta x}^{c_1/c}\right) & \frac{1}{2}\left(T_{\Delta x}^{c_{-1}/c}+T_{\Delta x}^{c_1/c}\right) & \frac{1}{6c}\left(T_{\Delta x}^{c_{-1}/c}-T_{\Delta x}^{c_1/c}\right) \\ \frac{c^2}{3}\left(T_{\Delta x}^{c_{-1}/c}-2T_{\Delta x}^{c_0/c}+T_{\Delta x}^{c_1/c}\right) & \frac{c}{2}\left(T_{\Delta x}^{c_{-1}/c}-T_{\Delta x}^{c_1/c}\right) & \frac{1}{6}\left(T_{\Delta x}^{c_{-1}/c}-4T_{\Delta x}^{c_0/c}+T_{\Delta x}^{c_1/c}\right) \end{bmatrix},$$

$$\boldsymbol{P}=\begin{bmatrix} \frac{(1-s_0)}{3}\left(T_{\Delta x}^{c_{-1}/c}+T_{\Delta x}^{c_0/c}+T_{\Delta x}^{c_1/c}\right) & \frac{(1-s_1)}{2c}\left(T_{\Delta x}^{c_{-1}/c}-T_{\Delta x}^{c_1/c}\right) & \frac{(1-s_2)}{6c^2}\left(T_{\Delta x}^{c_{-1}/c}-2T_{\Delta x}^{c_0/c}+T_{\Delta x}^{c_1/c}\right) \\ \frac{c(1-s_0)}{3}\left(T_{\Delta x}^{c_{-1}/c}-T_{\Delta x}^{c_1/c}\right) & \frac{(1-s_1)}{2}\left(T_{\Delta x}^{c_{-1}/c}+T_{\Delta x}^{c_1/c}\right) & \frac{(1-s_2)}{6c}\left(T_{\Delta x}^{c_{-1}/c}-T_{\Delta x}^{c_1/c}\right) \\ \frac{c^2(1-s_0)}{3}\left(T_{\Delta x}^{c_{-1}/c}-2T_{\Delta x}^{c_0/c}+T_{\Delta x}^{c_1/c}\right) & \frac{c(1-s_1)}{2}\left(T_{\Delta x}^{c_{-1}/c}-T_{\Delta x}^{c_1/c}\right) & \frac{(1-s_2)}{6}\left(T_{\Delta x}^{c_{-1}/c}-4T_{\Delta x}^{c_0/c}+T_{\Delta x}^{c_1/c}\right) \end{bmatrix},$$

$$\boldsymbol{Q}=\begin{bmatrix} \frac{s_0}{3}\left(T_{\Delta x}^{c_{-1}/c}+T_{\Delta x}^{c_0/c}+T_{\Delta x}^{c_1/c}\right) & \frac{s_1}{2c}\left(T_{\Delta x}^{c_{-1}/c}-T_{\Delta x}^{c_1/c}\right) & \frac{s_2}{6c^2}\left(T_{\Delta x}^{c_{-1}/c}-2T_{\Delta x}^{c_0/c}+T_{\Delta x}^{c_1/c}\right) \\ \frac{c}{3}\left(T_{\Delta x}^{c_{-1}/c}-T_{\Delta x}^{c_1/c}\right) & \frac{s_1}{2}\left(T_{\Delta x}^{c_{-1}/c}+T_{\Delta x}^{c_1/c}\right) & \frac{s_2}{6c}\left(T_{\Delta x}^{c_{-1}/c}-T_{\Delta x}^{c_1/c}\right) \\ \frac{c^2 s_0}{3}\left(T_{\Delta x}^{c_{-1}/c}-2T_{\Delta x}^{c_0/c}+T_{\Delta x}^{c_1/c}\right) & \frac{cs_1}{2}\left(T_{\Delta x}^{c_{-1}/c}-T_{\Delta x}^{c_1/c}\right) & \frac{s_2}{6}\left(T_{\Delta x}^{c_{-1}/c}-4T_{\Delta x}^{c_0/c}+T_{\Delta x}^{c_1/c}\right) \end{bmatrix},$$

then the characteristic polynomial $\mathcal{X}_{\boldsymbol{P}}$ of matrix $\boldsymbol{P}$ is written as

$$\mathcal{X}_{\boldsymbol{P}}=\gamma_3\boldsymbol{X}^3+\gamma_2\boldsymbol{X}^2+\gamma_1\boldsymbol{X}+\gamma_0\boldsymbol{I}, \tag{17}$$

where γ_i is given by

$$\begin{aligned}
\gamma_3&=T_{\Delta x}^{c_0/c},\\
\gamma_2&=\frac{s_2}{6}\left(T_{\Delta x}^{c_{-1}/c}+4T_{\Delta x}^{c_0/c}+T_{\Delta x}^{c_1/c}\right)+\frac{s_1}{2}\left(T_{\Delta x}^{c_{-1}/c}+T_{\Delta x}^{c_1/c}\right)\\
&\quad-\left(T_{\Delta x}^{c_{-1}/c}+T_{\Delta x}^{c_0/c}+T_{\Delta x}^{c_1/c}\right),\\
\gamma_1&=\frac{s_1s_2}{3}\left(T_{\Delta x}^{c_{-1}/c}+T_{\Delta x}^{c_0/c}+T_{\Delta x}^{c_1/c}\right)\\
&\quad-\frac{s_2}{6}\left(5T_{\Delta x}^{c_{-1}/c}+2T_{\Delta x}^{c_0/c}+5T_{\Delta x}^{c_1/c}\right)\\
&\quad-\frac{s_1}{2}\left(T_{\Delta x}^{c_{-1}/c}+2T_{\Delta x}^{c_0/c}+T_{\Delta x}^{c_1/c}\right)\\
&\quad+\left(T_{\Delta x}^{c_{-1}/c}+T_{\Delta x}^{c_0/c}+T_{\Delta x}^{c_1/c}\right),\\
\gamma_0&=-(1-s_1)(1-s_2)T_{\Delta x}^{c_0/c}.
\end{aligned} \tag{18}$$

Applying Eq. (16) recursively, we have

$$\boldsymbol{m}^{n+1}=\boldsymbol{P}^k\boldsymbol{m}^{n-k+1}+\sum_{l=0}^{k-1}\boldsymbol{P}^l\boldsymbol{Q}\boldsymbol{m}^{\mathrm{eq}|n-l},\ \forall k\in\mathbb{N}. \tag{19}$$

With the aid of the Cayley-Hamilton theorem [51], one can obtain $\sum_{k=0}^{k=3}\gamma_k\boldsymbol{P}^k=\boldsymbol{0}$ and rewrite above equation as

$$\boldsymbol{m}^{n+1}=-\sum_{k=0}^{2}\gamma_k\boldsymbol{m}^{n+k-2}+\sum_{k=0}^{3}\gamma_k\left(\sum_{l=0}^{k-2}\boldsymbol{P}^l\boldsymbol{Q}\boldsymbol{m}^{\mathrm{eq}|n+k-l-3}\right), \tag{20}$$

where $\boldsymbol{m}_1^n(x_j)=\phi_j^n:=\phi(j\Delta x,t_n)$. From Eq. (20), we can also derive the following finite-difference scheme:

$$\phi_j^{n+1}=-\sum_{k=0}^{2}\gamma_k\phi_j^{n+k-2}+\left[\sum_{k=0}^{2}\left(\sum_{l=0}^{k}\gamma_{3+l-k}\boldsymbol{P}^l\right)\boldsymbol{Q}\boldsymbol{m}_j^{\mathrm{eq}|n-k}\right]_1, \tag{21}$$

where $\boldsymbol{m}^{\mathrm{eq}|n}(x_j)$ is given by

$$\begin{aligned}
\boldsymbol{m}^{\mathrm{eq}}(j\Delta x,t_n)&=\boldsymbol{M}\boldsymbol{f}^{\mathrm{eq}}(j\Delta x,t_n)\\
&=\left(\phi_j^n,\phi_j^n u,[(1-3w_0)c^2+3u^2]\phi_j^n\right)^T.
\end{aligned}$$

Substituting Eq. (18) into Eq. (21) and after some manipulations, we can obtain the equivalent explicit FLFD scheme from the MRT-LB model (2),

$$\begin{aligned}
\phi_j^{n+1}&=\alpha_1\phi_j^n+\alpha_2\phi_{j-1}^n+\alpha_3\phi_{j+1}^n+\beta_1\phi_j^{n-1}+\beta_2\phi_{j-1}^{n-1}\\
&\quad+\beta_3\phi_{j+1}^{n-1}+\gamma\phi_j^{n-2}.
\end{aligned} \tag{22}$$

Here ϕ_j^n denotes $\phi(j\Delta x,t_n)$, $j\in\mathbb{Z}$, the parameters α_i, $\beta_i(i=1,2,3)$ and γ are given by

$$\begin{aligned}
\alpha_1&=1+s_2(w_0-1-\sigma^2),\\
\alpha_2&=1+\frac{s_1(\sigma-1)}{2}+\frac{s_2(\sigma^2-w_0)}{2},\\
\alpha_3&=1-\frac{s_1(\sigma+1)}{2}+\frac{s_2(\sigma^2-w_0)}{2},\\
\beta_1&=(w_0s_2-1)(1-s_1)-s_2(1-s_1)\sigma^2,\\
\beta_2&=\left[\frac{s_1(1-\sigma)}{2}-1\right](1-s_2)+\frac{s_2(w_0-\sigma^2)}{2}(s_1-1),\\
\beta_3&=\left[\frac{s_1(1+\sigma)}{2}-1\right](1-s_2)+\frac{s_2(w_0-\sigma^2)}{2}(s_1-1),\\
\gamma&=(1-s_1)(1-s_2),
\end{aligned} \tag{23}$$

where $\sigma=u/c$.

We point out that Eq. (22) is exactly equivalent to the MRT-LB model (2) for CDE (1), and the higher-order MRT-LB model and equivalent finite-difference scheme will be given in Sec. IV. In particular, if $u=0$, i.e., $\sigma=0$, then we can obtain a four-level finite-difference scheme for the diffusion equation from Eq. (22), and the parameters in Eq. (23) are simplified as

$$\begin{aligned}
&\alpha_1=1+s_2(w_0-1),\quad \alpha_2=\alpha_3=1-\frac{s_1}{2}-\frac{s_2w_0}{2},\\
&\beta_1=(w_0s_2-1)(1-s_1),\\
&\beta_2=\beta_3=\left(\frac{s_1}{2}-1\right)(1-s_2)+\frac{s_2w_0}{2}(s_1-1),\\
&\gamma=(1-s_1)(1-s_2).
\end{aligned} \tag{24}$$

It should be noted that Eq. (22) coupled with Eq. (24), as a special case of the present FLFD scheme, is the same as that reported in the previous work [8].

IV. THE ACCURACY AND STABILITY ANALYSIS

In this section, we will conduct a detailed theoretical analysis on the accuracy and stability of the MRT-LB model (2) and FLFD scheme (22). However, due to the equivalence between the MRT-LB model and FLFD scheme, for the sake of simplicity, we only focus on the FLFD scheme in the following analysis.

A. The accuracy of the four-level finite-difference scheme

We now pay our attention to the accuracy analysis of the FLFD scheme (22). To this end, we first apply the Taylor expansion to Eq. (22) at the position $x = j\Delta x$ and time t_n, and after some algebraic manipulations, one can obtain

$$\begin{aligned}
&\left(1+\sum_{i=1}^{3}\beta_i+2\gamma\right)\left[\frac{\partial\phi}{\partial t}\right]_j^n+(\alpha_2-\alpha_3+\beta_2-\beta_3)\frac{\Delta x}{\Delta t}\left[\frac{\partial\phi}{\partial x}\right]_j^n\\
&=\frac{\alpha_2+\alpha_3+\beta_2+\beta_3}{2}\frac{\Delta^2 x}{\Delta t}\left[\frac{\partial^2\phi}{\partial x^2}\right]_j^n+(\beta_2-\beta_3)\Delta x\left[\frac{\partial^2\phi}{\partial x\partial t}\right]_j^n+\frac{\sum_{i=1}^{3}\beta_i+4\gamma-1}{2}\Delta t\left[\frac{\partial^2\phi}{\partial t^2}\right]_j^n\\
&\quad+\frac{-\alpha_2+\alpha_3-\beta_2+\beta_3}{6}\frac{\Delta^3 x}{\Delta t}\left[\frac{\partial^3\phi}{\partial x^3}\right]_j^n+\frac{\beta_3-\beta_2}{2}\Delta x\Delta t\left[\frac{\partial^3\phi}{\partial x\partial t^2}\right]_j^n\\
&\quad-\frac{\beta_3+\beta_2}{2}\Delta^2 x\left[\frac{\partial^3\phi}{\partial x^2\partial t}\right]_j^n-\frac{\sum_{i=1}^{3}\beta_i+8\gamma+1}{6}\Delta^2 t\left[\frac{\partial^3\phi}{\partial t^3}\right]_j^n\\
&\quad+\frac{\alpha_2+\alpha_3+\beta_2+\beta_3}{24}\frac{\Delta^4 x}{\Delta t}\left[\frac{\partial^4\phi}{\partial x^4}\right]_j^n+\frac{\beta_2-\beta_3}{6}\Delta x\Delta^2 t\left[\frac{\partial^4\phi}{\partial x\partial t^3}\right]_j^n+\frac{\beta_2+\beta_3}{4}\Delta^2 x\Delta t\left[\frac{\partial^4\phi}{\partial x^2\partial t^2}\right]_j^n\\
&\quad+\frac{\beta_2-\beta_3}{6}\Delta^3 x\left[\frac{\partial^4\phi}{\partial x^3\partial t}\right]_j^n+\frac{\sum_{i=1}^{3}\beta_i+16\gamma-1}{24}\Delta^3 t\left[\frac{\partial^4\phi}{\partial t^4}\right]_j^n+\cdots.
\end{aligned}\tag{25}$$

Substituting Eq. (23) into the above equation and with the aid of the following relations derived from Eq. (25):

$$\begin{aligned}
\left[\frac{\partial^2\phi}{\partial x\partial t}\right]_j^n&=\kappa\left[\frac{\partial^3\phi}{\partial x^3}\right]_j^n-u\left[\frac{\partial^2\phi}{\partial x^2}\right]_j^n+O(\Delta^3 x+\Delta t\Delta x),\\
\left[\frac{\partial^2\phi}{\partial t^2}\right]_j^n&=\kappa^2\left[\frac{\partial^4\phi}{\partial x^4}\right]_j^n-2\kappa u\left[\frac{\partial^3\phi}{\partial x^3}\right]_j^n+u^2\left[\frac{\partial^2\phi}{\partial x^2}\right]_j^n+O(\Delta t),\\
\left[\frac{\partial^3\phi}{\partial x\partial t^2}\right]_j^n&=-2\kappa u\left[\frac{\partial^4\phi}{\partial x^4}\right]_j^n+u^2\left[\frac{\partial^3\phi}{\partial x^3}\right]_j^n+O(\Delta x),\\
\left[\frac{\partial^3\phi}{\partial x^2\partial t}\right]_j^n&=\kappa\left[\frac{\partial^4\phi}{\partial x^4}\right]_j^n-u\left[\frac{\partial^3\phi}{\partial x^3}\right]_j^n+O\left(\frac{\Delta^4 x}{\Delta t}+\Delta^2 x\right),\\
\left[\frac{\partial^3\phi}{\partial t^3}\right]_j^n&=3\kappa u^2\left[\frac{\partial^4\phi}{\partial x^4}\right]_j^n-u^3\left[\frac{\partial^3\phi}{\partial x^3}\right]_j^n+O\left(\frac{\Delta^2 x}{\Delta t}\right),\\
\left[\frac{\partial^4\phi}{\partial x\partial t^3}\right]_j^n&=-u^3\left[\frac{\partial^4\phi}{\partial x^4}\right]_j^n+O\left(\frac{1}{\Delta x}\right),\quad \left[\frac{\partial^4\phi}{\partial x^3\partial t}\right]_j^n=-u\left[\frac{\partial^4\phi}{\partial x^4}\right]_j^n+O(\Delta x),\\
\left[\frac{\partial^4\phi}{\partial x^2\partial t^2}\right]_j^n&=u^2\left[\frac{\partial^4\phi}{\partial x^4}\right]_j^n+O\left(\frac{\Delta^2 x}{\Delta t}\right),\quad \left[\frac{\partial^4\phi}{\partial t^4}\right]_j^n=u^4\left[\frac{\partial^4\phi}{\partial x^4}\right]_j^n+O\left(\frac{1}{\Delta t}\right),
\end{aligned}\tag{26}$$

we have

$$\left[\frac{\partial\phi}{\partial t}\right]_j^n+u\left[\frac{\partial\phi}{\partial x}\right]_j^n=\kappa\left[\frac{\partial^2\phi}{\partial x^2}\right]_j^n+\frac{uTR_3}{6s_1^2s_2}\Delta^2 x\left[\frac{\partial^3\phi}{\partial x^3}\right]_j^n+\frac{TR_4}{12s_1^3s_2}\frac{\Delta^4 x}{\Delta t}\left[\frac{\partial^4\phi}{\partial x^4}\right]_j^n+O(\Delta^2 t+\Delta^4 x+\Delta^2 x\Delta t).\tag{27}$$

At the diffusive scaling ($\Delta t \propto \Delta^2 x$), one can obtain an explicit FLFD scheme with the second-order accuracy in time and fourth-order accuracy in space once the following conditions are satisfied:

$$\varepsilon := (1-w_0)\Big(\frac{1}{s_1}-\frac{1}{2}\Big), \tag{28a}$$

$$TR_3 = 3w_0\big(s_1^2 - s_1^2 s_2 + 5s_1 s_2 - 4s_2 - 2s_1\big) + 2s_2\big(6 + s_1^2 - 6s_1\big) - \sigma^2 s_1(3s_2 + 3s_1 - s_1 s_2 - 6) = 0, \tag{28b}$$

$$\begin{aligned} TR_4 = {} & \frac{3}{2}(1-w_0)^2(s_1-2)\big(4s_1+4s_2-6s_1s_2+s_1^2s_2-2s_1^2\big) + \frac{1-w_0}{2}s_1(s_1-2)(6s_1+6s_2-s_1s_2-12) \\ & + \sigma^2 s_1\Big[30s_2(1-w_0) + 36(w_0+s_1+w_0s_1s_2-1) - 2s_1(16s_2+21w_0) \\ & + s_1^2\Big(\frac{13}{2}s_2-7\Big) + 3s_1^2w_0(4-3s_2)\Big] + \sigma^4 s_1^2\Big(6-5s_1-2s_2-5\frac{s_1s_2}{2}\Big) = 0. \end{aligned} \tag{28c}$$

In addition, we would also like to point out that when the parameters w_0, s_1, and s_2 satisfy Eqs. (28a), (28b), and (28c), the fourth-order MRT-LB model should also be obtained, which will be tested in Sec. V.

In the following, we give some remarks on above results.

Remark 1. We note that the relaxation parameter s_0 corresponding to the zeroth moment of distribution functions $f_i(x,t)$ (the conservative variable ϕ) does not appear in the finite-difference scheme (22), this means that it has no influence on the numerical results. This also explains why the relaxation parameter s_0 in the MRT-LB model can be chosen arbitrarily, which is consistent with the previous work [8]. In this sense, the MRT-LB model is identical to the TRT-LB model, and both of them give the same equivalent finite-difference scheme. However, unlike the relaxation parameter s_0, the relaxation parameter s_1 corresponding to the first-order moment of the distribution is related to the diffusion coefficient κ [see Eq. (28a)], and the relaxation parameter s_2 corresponding to the second-order moment of the distribution function has an important influence on the FLFD scheme (22) [see Eqs. (28b) and (28c)]. These similar results have also been reported on the MRT-LB model for diffusion equations [8].

Remark 2. If we consider the case with $u = 0$, then Eq. (1) will become a diffusion equation, and Eqs. (28b) and (28c) reduce to the results reported in Ref. [8]. Actually, if one continues to conduct the Taylor expansion to higher orders, then the scheme with the sixth-order accuracy in space [8] can also be obtained.

Remark 3. If we consider the SRT-LB model, i.e., $s_1 = s_2 := s$, then the condition (28) reduces to

$$\varepsilon = (1-w_0)\left(\frac{1}{s}-\frac{1}{2}\right), \tag{29a}$$

$$TR_3 = (6-6s+s^2)[-1+3(1-w_0)+\sigma^2] = 0, \tag{29b}$$

$$\begin{aligned} TR_4 = {} & (2-s)\{(12-12s+s^2)[1-w_0-2(1-w_0)^2] \\ & - s^2(1-w_0)^2\} + 3s\sigma^2[(1-w_0)(12s-s^2-12) \\ & + 2(s-1)(s^2-5s+5) + 3sw_0(s-1)(4-s)] \\ & + \sigma^4 s^2\frac{12-5s^2-14s}{2}. \end{aligned} \tag{29c}$$

It is obvious that Eqs. (29a) and (29b) are the same as those in Ref. [10], but Eq. (29c) is different unless $u = 0$, i.e., $\sigma = 0$. Actually, Straka [10] illustrated that the coefficient of the error term $\partial_x^4\phi$ is complicated and it is difficult to obtain the fourth-order cascaded SRT-LB model and equivalent finite-difference scheme. In our work, however, we consider the parametrs s_1, s_2, and w_0 as free parameters, and develop a fourth-order MRT-LB model when these parameters satisfy condition (28).

Remark 4. The diffusion coefficient κ in the FLFD scheme is same as that derived from the Chapman-Enskog expansion, which is due to the fact that a modified equilibrium distribution function with the parameter $\eta = 2(1-w_0)/w_0$ is adopted in the present MRT-LB model. However, when the popular equilibrium distribution function [12,15] is considered in the LB model, the recovered diffusion coefficient would have a redundant part which is dependent on the velocity u [15]. Moreover, the velocity-dependant diffusion term also has some influences and limitations on the selection of parameters in numerical experiments.

Remark 5. To preserve the fourth-order accuracy of MRT-LB model and FLFD scheme, the initial condition of distribution function $f_i(x,t)$ in the MRT-LB model and initial value of $\phi(x,t)$ in FLFD scheme must be given properly. According to the previous work [32], we utilize the following expression to initialize the distribution function f_i in implementing the MRT-LB model:

$$\boldsymbol{f} = \boldsymbol{f}^{\rm eq} - \Delta t(\boldsymbol{M}^{-1}\boldsymbol{S}\boldsymbol{M})^{-1}\mathcal{D}\boldsymbol{f}^{\rm eq}, \tag{30}$$

where $\mathcal{D} = \mathbf{diag}(D_0, D_1, D_{-1})$, $D_i = \partial_t + c_i\partial_x$. Additionally, it should be noted that with the help of Eq. (1), the term $\partial_t\phi$ appeared in Eq. (30) can be replaced by the spatial derivatives of scalar variable ϕ, which can be further determined from the initial condition. However, in the implementation of the FLFD scheme, the values of the variable ϕ at the first three time levels are needed. Thus, in addition to the initial condition, one must adopt some other numerical schemes to obtain the values of variable ϕ at the second and third time levels. The inclusion of the extra time levels also brings a larger memory requirement to store the variable ϕ.

Finally, for the MRT-LB model and FLFD scheme, we must determine the weight coefficient w_0, the relation parameters s_1 and s_2 from Eq. (28) for the specified σ and ε (or u and κ). Due to the nonlinearity and coupling among Eqs. (28a), (28b), and (28c), it is difficult to derive the explicit expressions of w_0, s_1 and s_2 in terms of κ and σ, and some numerical

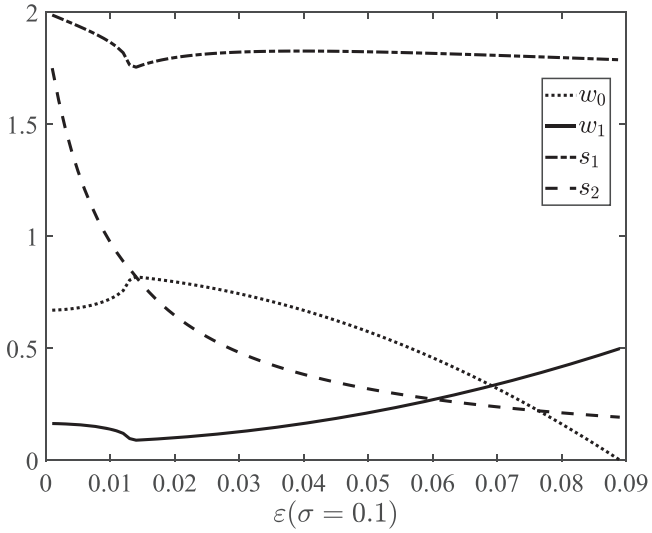

FIG. 1. The weight coefficients w_0, w_1, the relaxation parameters s_1 and s_2 as a function of the parameter ε ($\sigma = 0.1$).

methods must be adopted. Actually, the solution of condition (28) is not unique, for this reason, we numerically solve the condition (28) and only consider one of the solutions to obtain w_0, s_1, and s_2 through fixing the parameter ε ($0 < \varepsilon \leqslant 0.09$), and plot the result in Fig. 1, where $\sigma = 0.1$. It should be noted that if one considers all the solutions of the condition (28) with the parameter $\sigma \in (0, 1)$ fixed, the max value of the parameter ε can be reached is about 0.35 (see details in Fig. 2). As shown in Fig. 1, the parameters w_0 and s_2 all satisfy the conditions of $0 < w_0 < 1$ and $0 < s_1, s_2 < 2$.

B. The stability analysis

In this part, we will give a necessary and sufficient condition for the stability of the MRT-LB model and FLFD scheme. According to the Corollary 10 in Ref. [51], the MRT-LB model (2) is stable if and only if the corresponding FLFD scheme (22) is stable in the von Neumann sense. For this reason, here we just focus on the stability condition of the FLFD scheme, and obtain the following proposition.

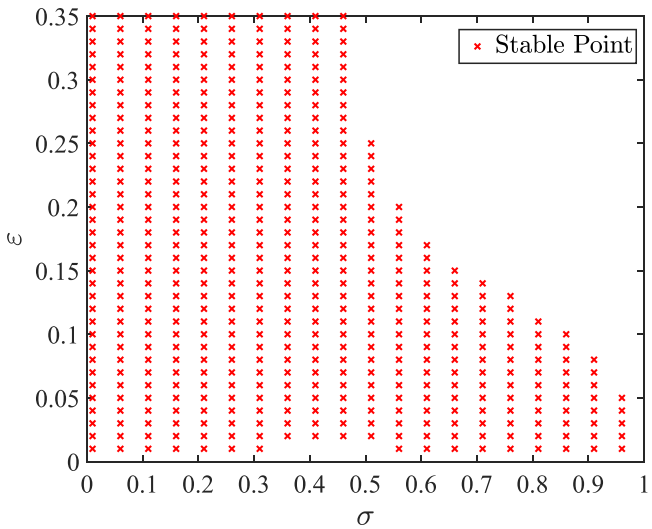

FIG. 2. The stability region of the fourth-order MRT-LB model and FLFD scheme.

Proposition. The MRT-LB model (2) and FLFD scheme (22) are stable if and only if $\sigma \leqslant 1$ (CFL condition), $0 < s_1, s_2 < 2$ and the following constraints hold:

$$\begin{aligned}\max_{\omega\in[-1,1]} \big\{&(1-\omega^2)^2\sigma^4\big(A_{s_1}^2 s_1^2 - \Omega_{s_1}^2\big)\Omega_{s_1}^2 \\ &+ (1-\omega^2)\sigma^2\big(\Omega_{s_1}^2\big[B^2 + 2\big(O_2^2 - O_1^2\big)\big] \\ &- 4s_1A_{s_1}\Omega_{s_1}BO_2 + s_1^2A_{s_1}^2(O_1+O_2)^2\big) \\ &+ (O_1-O_2)^2[B^2 - (O_1+O_2)^2]\big\} \leqslant 0, \end{aligned} \tag{31}$$

where

$$\begin{aligned} &A = (w_0 - \sigma^2)(\omega - 1) + 1, \\ &\Omega = (1-s_1)(1-s_2), \\ &A_{s_1} = 1 - \frac{\Omega^2}{s_1 - 1}, \quad A_{s_2} = 1 - \frac{\Omega^2}{s_2 - 1}, \\ &C_{s_1} = \left(1 + \frac{\Omega^2}{s_1 - 1}\right)(2 - s_1), \\ &\Omega_{s_1} = s_1(2-s_1)(1-s_2), \quad \Omega_{s_2} = s_2(2-s_2)(1-s_1), \\ &O_1 = \Omega_{s_1}\omega + \Omega_{s_2}A, \quad O_2 = 1 - \Omega^2, \\ &B = C_{s_1}\omega - AA_{s_2}s_2 + O_2. \end{aligned} \tag{32}$$

Proof. From the FLFD scheme (22), one can obtain its amplification matrix $\boldsymbol{G}$ as

$$\boldsymbol{G} = \begin{pmatrix} \alpha_1 + \alpha_2 e^{-i\theta} + \alpha_3 e^{i\theta} & \beta_1 + \beta_2 e^{-i\theta} + \beta_3 e^{i\theta} & \gamma \\ 1 & 0 & 0 \\ 0 & 1 & 0 \end{pmatrix}, \tag{33}$$

and the characteristic polynomial can be expressed as

$$p(\lambda) = \lambda^3 + a_2\lambda^2 + a_1\lambda + a_0, \tag{34}$$

where the coefficients a_0, a_1, a_2 are given by

$$\begin{aligned} &a_0 = (1-s_1)(s_2 - 1), \quad |a_0| < 1, \\ &a_1 = s_2(1-s_1)(w_0 - \sigma^2)(\cos\theta - 1) + (1-s_2)(2-s_1) \\ &\qquad \times \cos\theta + (1-s_1) + s_1(1-s_2)\sigma i \sin\theta, \\ &a_2 = s_2(w_0 - \sigma^2)(\cos\theta - 1) + (s_2 - 1) + (s_1 - 2) \\ &\qquad \times \cos\theta - s_1\sigma i \sin\theta. \end{aligned} \tag{35}$$

In order to find the constraint conditions to ensure the roots of the characteristic polynomial (34) denoted by λ_k ($k = 1, 2, 3$) satisfy:

1. $|\lambda_k| \leqslant 1$;
2. If $|\lambda_k| = 1$, then λ_k is a simple eigenvalue of $\boldsymbol{G}$.

Now we divide the derivation process into following three steps.

Step 1. We first define two polynomials as

$$p^*(\lambda) = a_0\lambda^3 + \overline{a}_1\lambda^2 + \overline{a}_2\lambda + 1, \tag{36a}$$

$$\begin{aligned} p_1(\lambda) &= \frac{p^*(0)p(\lambda) - p(0)p^*(\lambda)}{\lambda} \\ &= (1 - |a_0|^2)\lambda^2 + (a_2 - a_0\overline{a}_1)\lambda + (a_1 - a_0\overline{a}_2), \end{aligned} \tag{36b}$$

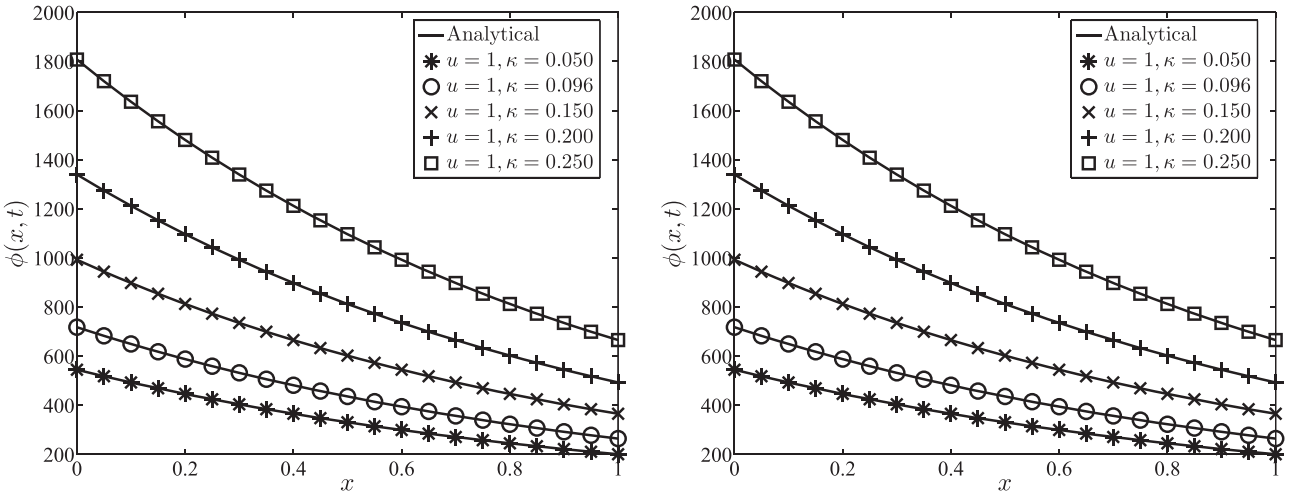

(a) MRT-LB model (b) FLFD scheme

FIG. 3. The numerical and analytical solutions under different values of diffusion coefficient κ ($u = 1$).

where $\overline{a}_i$ is the conjugate complex of a_i, and

$$
\begin{aligned}
1 - |a_0|^2 &= 1 - (1 - s_1)^2(1 - s_2)^2 = O_2, \\
a_2 - a_0\overline{a}_1 &= s_2[1 - (1 - s_1)^2(s_2 - 1)][(w_0 - \sigma^2)(\cos\theta - 1) + 1] \\
&\quad + [1 + (s_1 - 1)(s_2 - 1)^2](s_1 - 2)\cos\theta + [(1 - s_1)^2(1 - s_2)^2 - 1] - i[1 + (1 - s_1)^2(1 - s_2)]\sigma\sin\theta \\
&= As_2A_{s_2} - C_{s_1}\cos\theta - O_2 - is_1\sigma A_{s_1}\sin\theta, \\
a_1 - a_0\overline{a}_2 &= s_2(2 - s_2)(1 - s_1)[(w_0 - \sigma^2)(\cos\theta - 1) + 1] + s_1(1 - s_2)(2 - s_1)(\cos\theta + i\sigma\sin\theta) \\
&= \Omega_{s_2}A + \Omega_{s_1}(\cos\theta + i\sigma\sin\theta).
\end{aligned} \tag{37}
$$

From Eqs. (34), (35), and (36a), we can obtain $|p^*(0)| > |p(0)|$ under the condition of $0 < s_1, s_2 < 2$. Following the Theorem 6.1 in Ref. [56], we can show that the characteristic polynomial $p(\lambda)$ (34) is a von Neumann polynomial if and only if $p_1(\lambda)$ (36b) is a von Neumann polynomial.

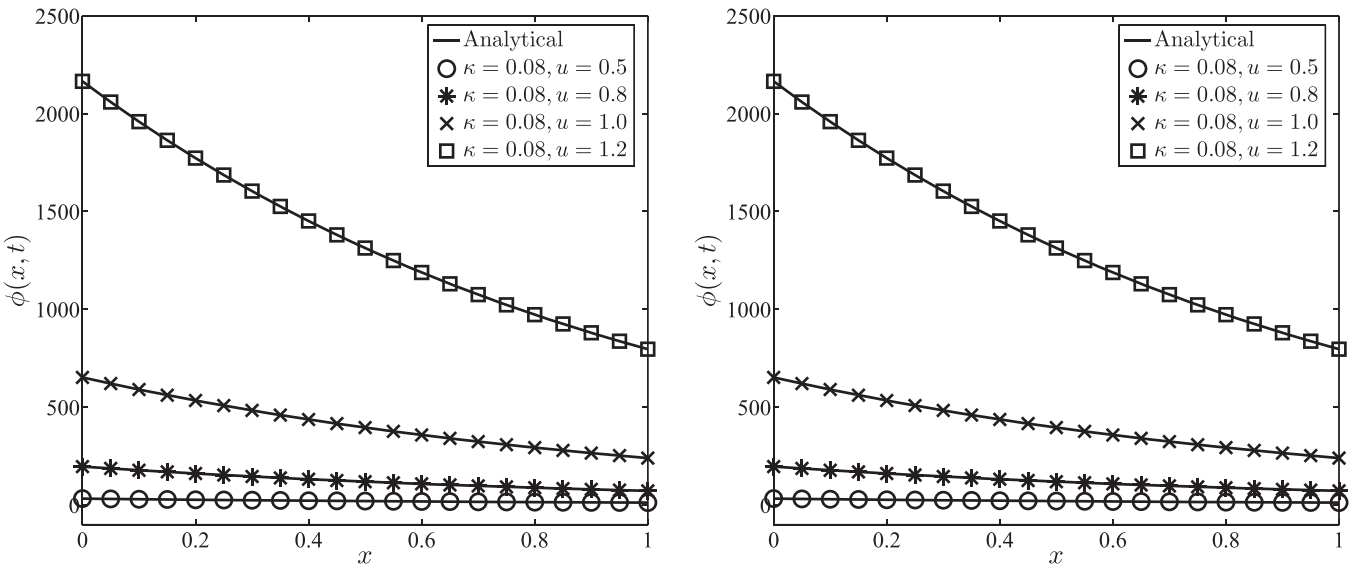

(a) MRT-LB model (b) FLFD scheme

FIG. 4. The numerical and analytical solutions under different values of velocity u ($\kappa = 0.08$).

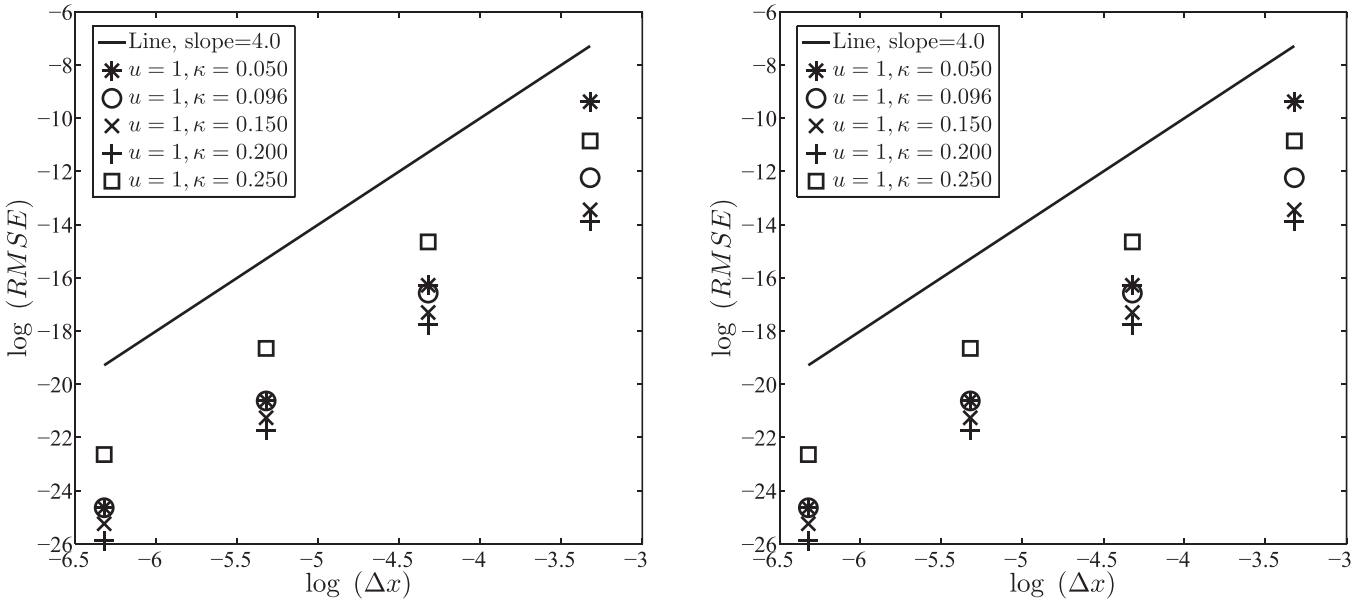

(a) MRT-LB model (b) FLFD scheme

FIG. 5. The convergence rates of MRT-LB model and FLFD scheme with different values of diffusion coefficient κ ($u = 1$).

Step 2. Similarly to $p(\lambda)$ (34), we also introduce the another two polynomials based on $p_1(\lambda)$ (36b),

$$p_1^*(\lambda) = (\bar{a}_1 - a_0 a_2)\lambda^2 + (\bar{a}_2 - a_0 a_1)\lambda + (1 - |a_0|^2), \tag{38a}$$

$$p_2(\lambda) = \frac{p_1^*(0)p(\lambda) - p_1(0)p_1^*(\lambda)}{\lambda} = [(1 - |a_0|^2)^2 - |a_1 - a_0\bar{a}_2|^2]\lambda + [(1 - |a_0|^2)(a_2 - a_0\bar{a}_1) - (a_1 - a_0\bar{a}_2)(\bar{a}_2 - a_0 a_1)]. \tag{38b}$$

In the following, we will show $|p_1^*(0)| > |p_1(0)|$. From Eq. (37) one can obtain

$$|a_1 - a_0\bar{a}_2| < |\Omega_{s_1}| + |\Omega_{s_2}| = s_2(2 - s_2)|1 - s_1| + s_1(2 - s_1)|1 - s_2|, \tag{39}$$

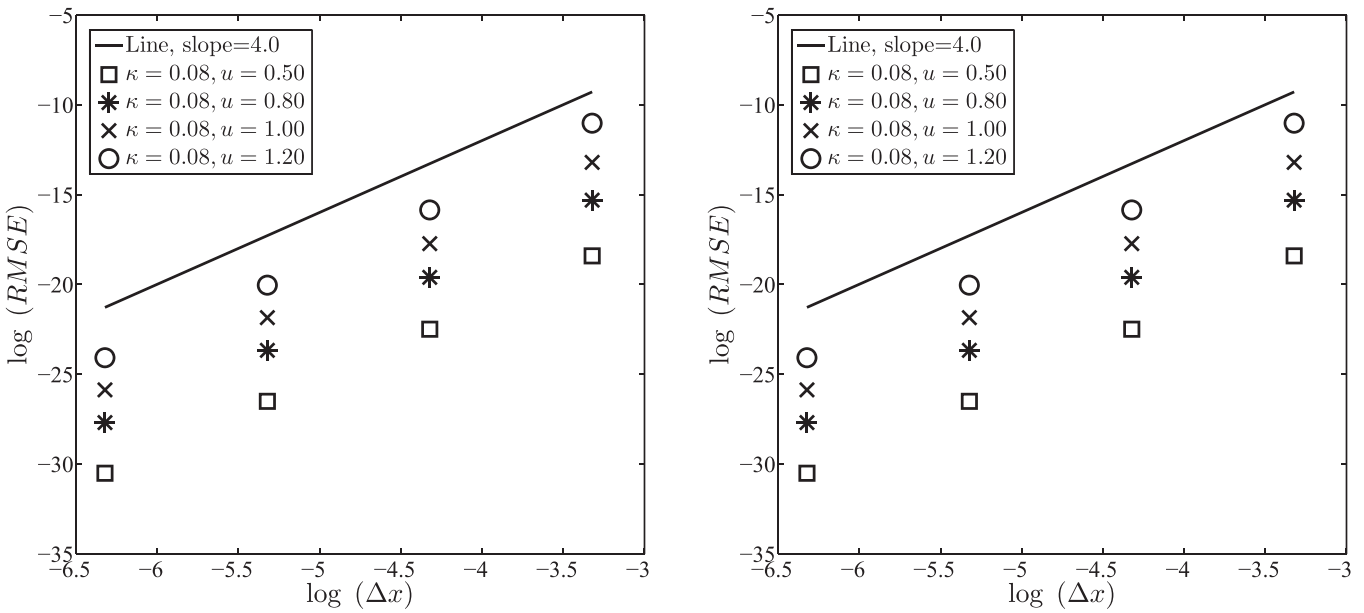

(a) MRT-LB model (b) FLFD scheme

FIG. 6. The convergence rates of MRT-LB model and FLFD scheme under different values of velocity u ($\kappa = 0.08$).

TABLE I. The RMSEs and CRs of MRT-LB model and FLFD scheme under different values of velocity u ($\kappa = 0.1$).

κ	u	Δx	Δt	$\mathrm{RMSE}_{\Delta x,\Delta t}$	$\mathrm{RMSE}_{\Delta x/2,\Delta t/4}$	$\mathrm{RMSE}_{\Delta x/4,\Delta t/16}$	$\mathrm{RMSE}_{\Delta x/8,\Delta t/64}$	CR
0.08	0.5	1/10	1/50	2.8584×10^{-6}	1.6839×10^{-7}	1.0430×10^{-8}	6.4843×10^{-10}	~4.0290
0.08	0.8	1/10	1/50	2.4502×10^{-5}	1.2460×10^{-6}	7.4375×10^{-8}	4.5899×10^{-9}	~4.1274
0.08	1.0	1/10	1/50	1.0513×10^{-4}	4.5823×10^{-6}	2.6359×10^{-7}	1.6166×10^{-8}	~4.2238
0.08	1.2	1/10	1/50	4.7805×10^{-4}	1.6812×10^{-5}	9.2182×10^{-7}	5.5906×10^{-8}	~4.3505
0.05	1	1/10	1/25	1.5001×10^{-3}	1.2567×10^{-5}	6.2255×10^{-7}	3.8219×10^{-8}	~5.0947
0.096	1	1/10	1/50	2.0708×10^{-4}	1.0236×10^{-5}	6.1765×10^{-7}	3.8448×10^{-8}	~4.1320
0.15	1	1/10	1/200	8.9667×10^{-5}	6.1834×10^{-6}	3.9851×10^{-7}	2.5236×10^{-8}	~3.9296
0.20	1	1/10	1/200	6.6506×10^{-5}	4.5042×10^{-6}	2.8891×10^{-7}	1.6191×10^{-8}	~4.0127
0.25	1	1/10	1/100	5.3815×10^{-4}	3.8889×10^{-5}	2.4274×10^{-6}	1.5257×10^{-7}	~3.9273

where $0 < w_0 < 1$, $|\sigma| \leqslant 1$ and $|\cos\theta| \leqslant 1$ are used. To prove $|p_1^*(0)| > |p_1(0)|$, the following four cases are needed to be verified:

$$\text{Case 1}: \Omega_{s_1} + \Omega_{s_2} < 1 - \Omega^2, \quad 0 < s_1 \leqslant 1, \quad 0 < s_2 \leqslant 1, \tag{40a}$$

$$\text{Case 2}: -\Omega_{s_1} - \Omega_{s_2} < 1 - \Omega^2, \quad 1 \leqslant s_1 < 2, \quad 1 \leqslant s_2 < 2, \tag{40b}$$

$$\text{Case 3}: \Omega_{s_1} - \Omega_{s_2} < 1 - \Omega^2, \quad 0 < s_1 \leqslant 1, \quad 1 \leqslant s_2 < 2, \tag{40c}$$

$$\text{Case 4}: -\Omega_{s_1} + \Omega_{s_2} < 1 - \Omega^2, \quad 1 \leqslant s_1 < 2, \quad 0 < s_2 \leqslant 1. \tag{40d}$$

We now consider the Case 1, and to this end a function g dependent on s_1 and s_2 is first introduced,

$$g(s_1, s_2) = 1 - \Omega^2 - \Omega_{s_1} - \Omega_{s_2}, \quad 0 < s_1 \leqslant 1, \quad 0 < s_2 \leqslant 1, \tag{41}$$

from which it is clear that $g(s_1, s_2) > \inf\{g(s_1, s_2), (s_1, s_2) \in (0, 1] \times (0, 1]\} = 0$. The analysis of the other three cases in Eq. (40) are similar and not shown here. In this way, we obtain the result $|p_1^*(0)| > |p_1(0)|$, which indicates the characteristic polynomial $p(\lambda)$ (34) is a von Neumann polynomial if and only if $p_2(\lambda)$ (38b) is a von Neumann polynomial [56].

Step 3. Based on steps 1 and 2, we now pay attention to the polynomial $p_2(\lambda)$ (38b) [the degree of polynomial $p_2(\lambda)$ is equal to unity], and it is a von Neumann polynomial iff

$$|(1 - |a_0|^2)(a_2 - a_0\bar{a}_1) - (a_1 - a_0\bar{a}_2)(\bar{a}_2 - a_0 a_1)| \leqslant (1 - |a_0|^2)^2 - |a_1 - a_0\bar{a}_2|^2. \tag{42}$$

To facilitate our analysis, we split the real and imaginary parts of these complex numbers as follows:

$$1 - |a_0|^2 = O_2 = a_r, \quad a_2 - a_0\bar{a}_1 = a_{r11} + ia_{r12}, \quad a_1 - a_0\bar{a}_2 = a_{r21} + ia_{r22}, \tag{43}$$

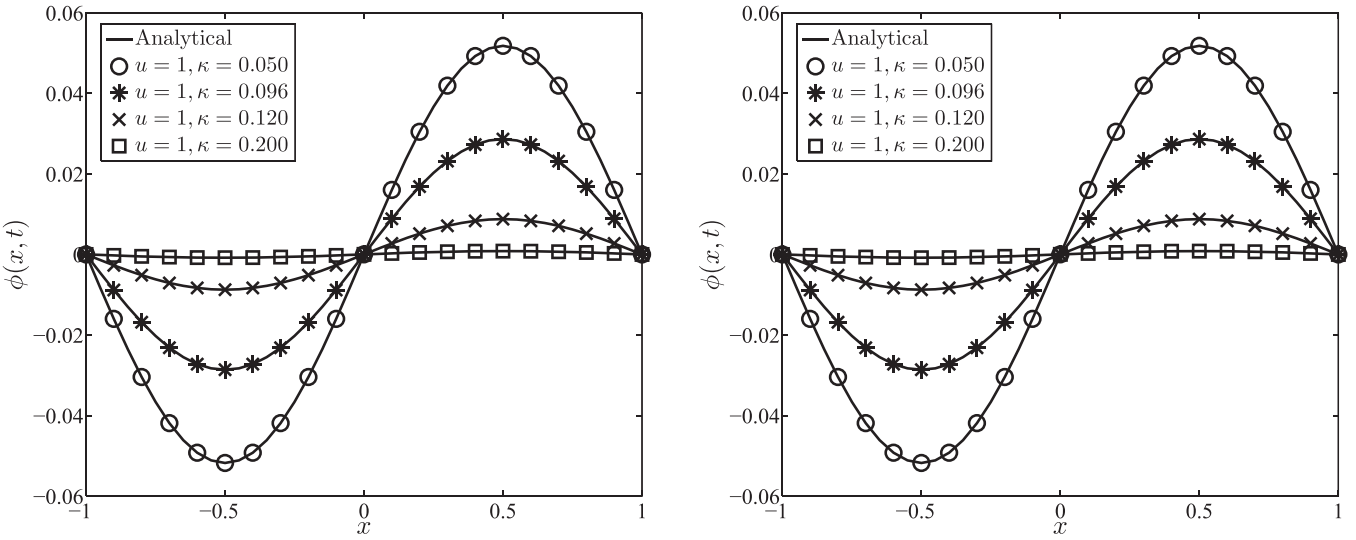

(a) MRT-LB model (b) FLFD scheme

FIG. 7. The numerical and analytical solutions under different values of diffusion coefficient κ ($u = 1$).

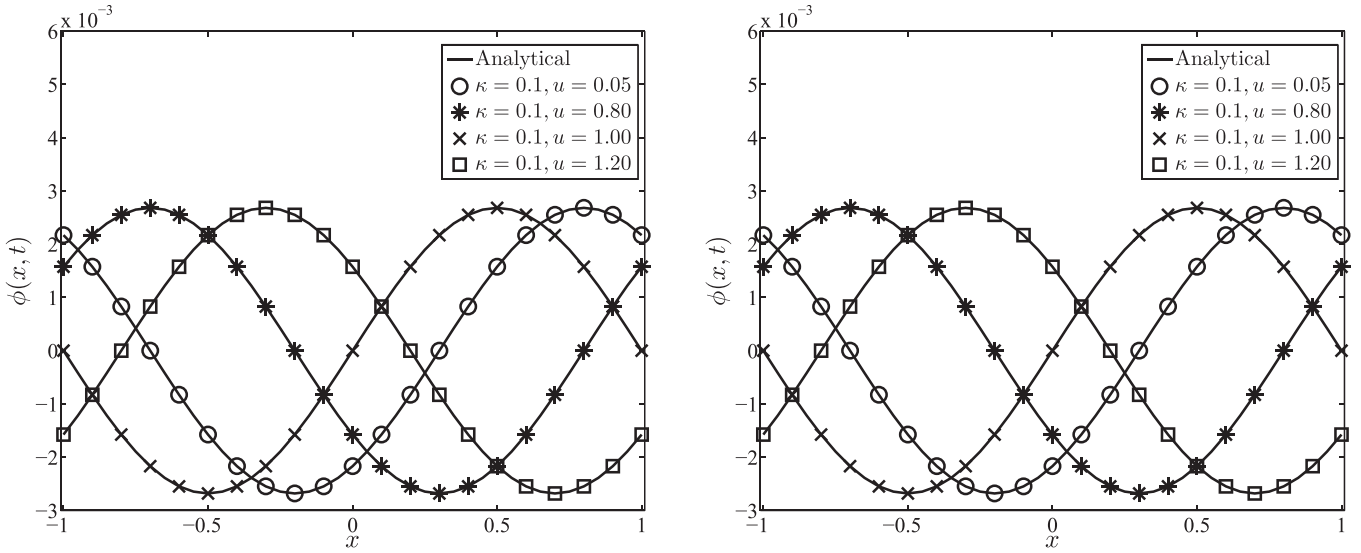

(a) MRT-LB model (b) FLFD scheme

FIG. 8. The numerical and analytical solutions under different values of velocity u ($\kappa = 0.1$).

where $a_r, a_{r11}, a_{r12}, a_{r21}$ and $a_{r22} \in \mathbb{R}$. Then Eq. (42) can be written equivalently as

$$(a_r a_{r11} - a_{r21}a_{11} - a_{r22}a_{r12})^2 + (a_r a_{r12} + a_{r21}a_{r12} - a_{r22}a_{r11})^2 - \left(a_r^2 - a_{r21}^2 - a_{r22}^2\right)^2 \leqslant 0. \tag{44}$$

Based on Eqs. (32) and (44) and after some manipulations, Eq. (42) becomes

$$\begin{aligned}&\left[-s_1\sigma A_{s_1}\sin\theta\left(\Omega_{s_1}\cos\theta + A\Omega_{s_2} + 1 - \Omega^2\right) + \Omega_{s_1}\sigma\sin\theta\left(C_{s_1}\cos\theta - AA_{s_2}s_2 + 1 - \Omega^2\right)\right]^2\\ &\quad - \left[\left(\Omega_{s_1}\cos\theta + A\Omega_{s_2}\right)^2 - (1-\Omega^2)^2 + \Omega_{s_1}^2\sigma^2\sin^2\theta\right]^2 + \left[A_{s_1}\Omega_{s_1}s_1\sigma^2\sin^2\theta\right.\\ &\quad \left. + \left[\Omega_{s_1}\cos\theta + A\Omega_{s_2} - (1-\Omega^2)\right]\left(C_{s_1}\cos\theta - AA_{s_1}s_2 + 1 - \Omega^2\right)\right]^2 \leqslant 0.\end{aligned} \tag{45}$$

Through observing the structure and terms of Eq. (45), we have the following formula:

$$\begin{aligned}&\sigma^4\Omega_s^2\sin^4\theta\left(A_{s_1}^2 s_1^2 - \Omega_{s_1}^2\right) + \sigma^2\sin^2\theta\left\{\Omega_{s_1}^2\left[B^2 + 2\left(O_2^2 - O_1^2\right)\right] - 4s_1A_{s_1}\Omega_{s_1}BO_2 + s_1^2A_{s_1}^2(O_1+O_2)^2\right\}\\ &\quad + (O_1 - O_2)^2[B^2 - (O_1+O_2)^2] \leqslant 0.\end{aligned} \tag{46}$$

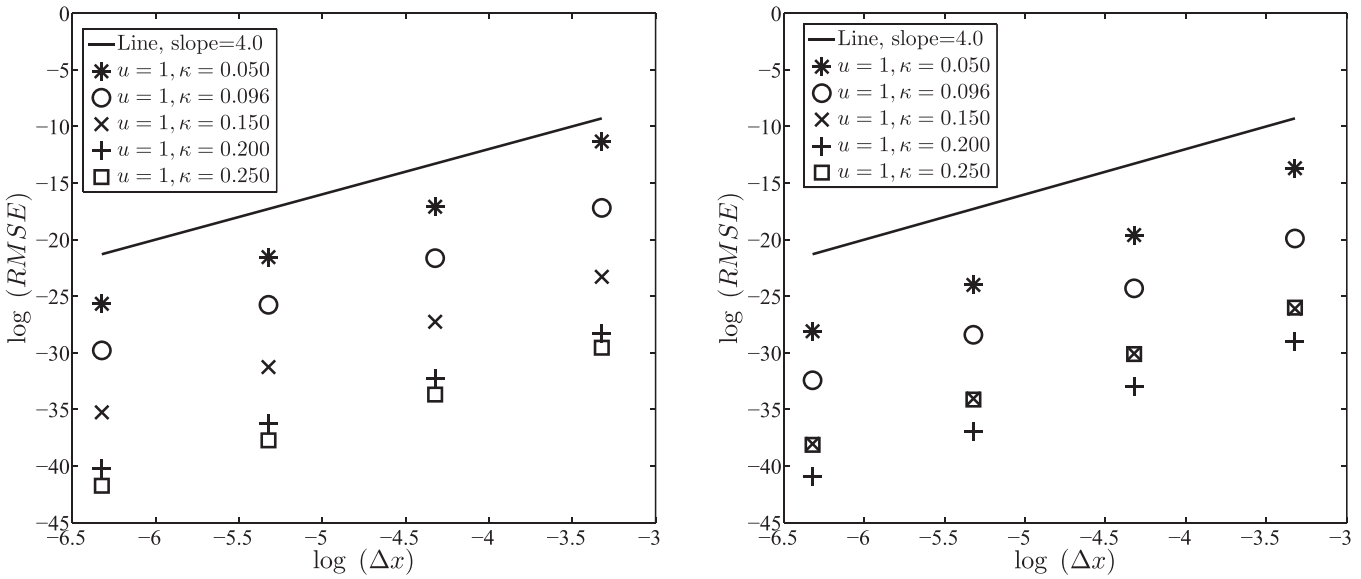

(a) MRT-LB model (b) FLFD scheme

FIG. 9. The convergence rates of MRT-LB model and FLFD scheme under different values of diffusion coefficient κ ($u = 1$).

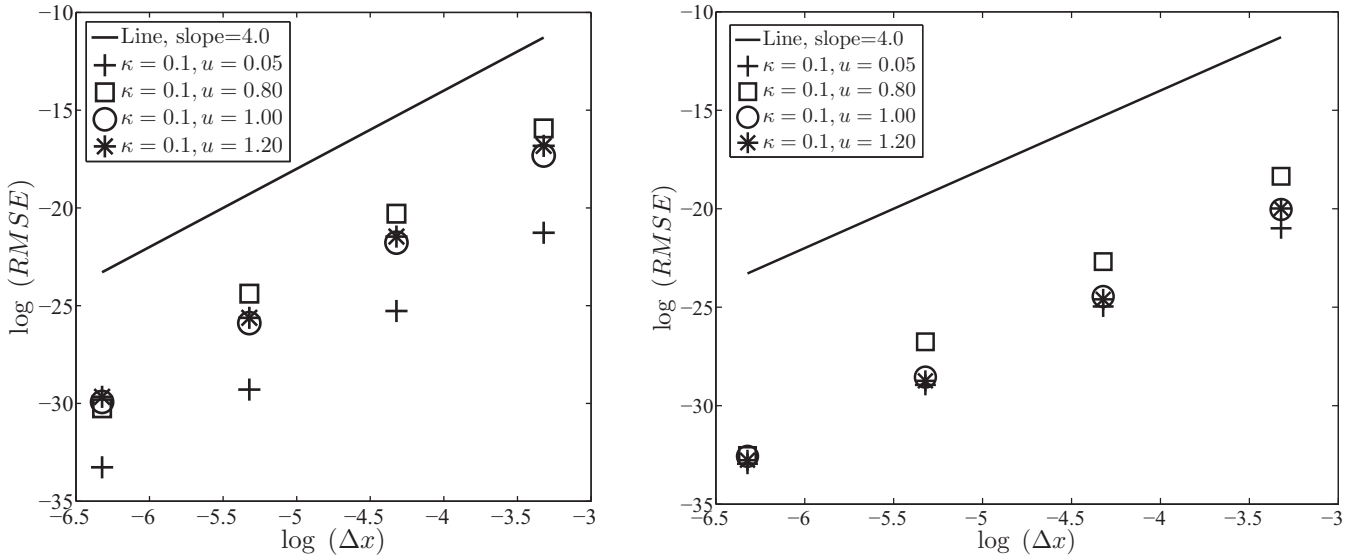

(a) MRT-LB model

(b) FLFD scheme

FIG. 10. The convergence rates of MRT-LB model and FLFD scheme under different values of velocity u ($\kappa = 0.1$).

To make the formula look more concise, we define $\cos\theta = \omega$, and obtain the necessary and sufficient conditions, i.e., Eq. (31), to ensure the MRT-LB model and FLFD scheme stable. ■

We now present some discussion on two special cases of the present MRT-LB model.

Remark 6. For the stability analysis, Ginzburg *et al.* [57] defined an evolution matrix $\boldsymbol{L} := \boldsymbol{K}(\boldsymbol{I} + \boldsymbol{C})$ with $\boldsymbol{K} := \mathbf{diag}(1, e^{-i\theta}, e^{-i\theta})$. In the present work, we can obtain the evolution matrix $\boldsymbol{L}$ through combining the parameters s_1, s_2 and σ,

$$\boldsymbol{L} = \begin{Bmatrix} \alpha_1 & -\xi & -\xi \\ \frac{1}{2}(s_2 + \xi + s_1\sigma)e^{-i\theta} & \alpha_2 e^{-i\theta} & \frac{1}{2}[\xi + s_1(1+\sigma)]e^{-i\theta} \\ \frac{1}{2}(s_2 + \xi - s_1\sigma)e^{i\theta} & \frac{1}{2}[\xi - s_1(\sigma - 1)]e^{i\theta} & \alpha_3 e^{i\theta} \end{Bmatrix}, \tag{47}$$

where $\xi = s_2(\sigma^2 - w_0)$. It is easy to show that the characteristic polynomial of matrix $\boldsymbol{L}$ is identical to that of the matrix $\boldsymbol{G}$ [see Eq. (33)]. Thus, one can directly conclude that the relaxation parameters s_1 and s_2 satisfying $(1/s_1 - 1/2)(1/s_2 - 1/2) = 1/4$ is the optimal stability condition [58].

Remark 7. It is obvious that both the fourth-order condition (28) and stability condition (31) are nonlinear, and it is difficult to determine the stability region of the fourth-order MRT-LB model and FLFD scheme. For this reason, we only consider the stability region in a numerical way. As seen in Fig. 2, one can find that the range of the parameter ε decreases as σ approaches to 1.

Case 1. $s_2 = 1$. In this case, the following stability condition can be derived from Eq. (31):

$$\begin{aligned} \max_{\omega\in[-1,1]} \big\{ & s_1^2\sigma^2(1+\omega)(1+O_1)^2 \\ & + (2-s_1)(1-O_1)(1-w_0+\sigma^2)\big[(2-s_1) \\ & \times (1-w_0+\sigma^2)(1-\omega)(1-O_1) + 2\big(O_1^2 - 1\big)\big]\big\} \\ \leqslant\ & 0, \end{aligned} \tag{48}$$

which is same as Proposition 12 in the previous work [51].

Case 2. $u = 0$. Under this condition, Eq. (1) becomes a diffusion equation, and one can find the corresponding

TABLE II. The RMSEs and CRs of the MRT-LB model under different values of velocity u ($\kappa = 0.1$).

κ	u	Δx	Δt	$\mathrm{RMSE}_{\Delta x,\Delta t}$	$\mathrm{RMSE}_{\Delta x/2,\Delta t/4}$	$\mathrm{RMSE}_{\Delta x/4,\Delta t/16}$	$\mathrm{RMSE}_{\Delta x/8,\Delta t/64}$	CR
0.1	0.05	1/10	1/50	3.9504×10^{-7}	2.4691×10^{-8}	1.5233×10^{-9}	9.6884×10^{-11}	∼3.9978
	0.80	1/10	1/50	1.6002×10^{-5}	7.7646×10^{-7}	4.5602×10^{-8}	7.8503×10^{-10}	∼4.7717
	1.00	1/10	1/50	6.1075×10^{-6}	2.7842×10^{-7}	1.6065×10^{-8}	9.8280×10^{-10}	∼4.2005
	1.20	1/10	1/50	8.6006×10^{-6}	3.4486×10^{-7}	1.9362×10^{-8}	1.1781×10^{-9}	∼4.2779

TABLE III. The RMSEs and CRs of the FLFD scheme under different values of velocity u ($\kappa = 0.1$).

κ	u	Δx	Δt	$\mathrm{RMSE}_{\Delta x,\Delta t}$	$\mathrm{RMSE}_{\Delta x/2,\Delta t/4}$	$\mathrm{RMSE}_{\Delta x/4,\Delta t/16}$	$\mathrm{RMSE}_{\Delta x/8,\Delta t/64}$	CR
0.1	0.05	1/10	1/50	4.8000×10^{-7}	3.0581×10^{-8}	1.9408×10^{-9}	1.2082×10^{-10}	∼3.9853
	0.80	1/10	1/50	2.9912×10^{-6}	1.4824×10^{-7}	8.8110×10^{-9}	1.6126×10^{-10}	∼4.7263
	1.00	1/10	1/50	9.2846×10^{-7}	4.3442×10^{-8}	2.5454×10^{-9}	1.5684×10^{-10}	∼4.1771
	1.20	1/10	1/50	9.6321×10^{-7}	3.9317×10^{-8}	2.2348×10^{-9}	1.3669×10^{-10}	∼4.2609

MRT-LB model (or FLFD scheme) is unconditionally stable, which is consistent with the result in Ref. [8].

The detailed discussion on above two cases can be found in the Appendix.

V. NUMERICAL RESULTS AND DISCUSSION

In this section, we conduct some simulations to test the present MRT-LB model and FLFD scheme, the weight coefficient w_0, the relaxation parameters s_1 and s_2 are determined from condition (28), and the parameters σ and ε are chosen based on the stability region shown in Fig. 2. To measure the accuracy of the MRT-LB model and FLFD scheme, the following root-mean-square error (RMSE) is adopted [5]:

$$\mathrm{RMSE} = \sqrt{\frac{\sum_{j=1}^{N_x}[\phi(j\Delta x, n\Delta t) - \phi^*(j\Delta x, n\Delta t)]^2}{N_x}}, \quad (49)$$

where N_x is the number of grid points, $\Delta x = L/N_x$ is lattice size (L is characteristic length), ϕ and ϕ^* are the numerical and analytical solutions, respectively. Based on the definition of RMSE, one can estimate the convergence rate (CR) of numerical scheme with the following formula:

$$\mathrm{CR} = \frac{\log(\mathrm{RMSE}_{\Delta x}/\mathrm{RMSE}_{\Delta x/2})}{\log 2}. \quad (50)$$

In order to ensure the MRT-LB scheme and FLFD scheme have a fourth convergence rate, and due to the complexity of the conditions to ensure the MRT-LB model and FLFD scheme be fourth-order accurate and stable, we note that we can first determine a set of parameters in terms of the parameter and to satisfy the fourth-order condition Eq. (26), and then verify whether this set of parameters satisfy the stability condition Eq. (29) or not. And the following numerical simulations in Sec. V are carried out under this premise.

Example 1. We first consider the CDE (1) with the following initial and boundary conditions:

$$\begin{aligned} &\phi(x,0) = e^{-x}, \quad 0 \leqslant x \leqslant 1, \\ &\phi(0,t) = e^{(u+\kappa\times 1)t}, \quad \phi(1,t) = e^{-1+(u+\kappa\times 1)t}, \quad t > 0, \end{aligned} \quad (51)$$

and obtain the analytical solution of this problem as

$$\phi(x,t) = e^{-x+(u+\kappa\times 1)t}. \quad (52)$$

In the MRT-LB model with the D1Q3 lattice structure, one can obtain the distribution functions f_0 and f_1 (or f_{-1}) at boundary nodes in the propagation step, then the last one distribution function f_i can be computed accurately with the aid of Eq. (7) under the Dirichlet boundary condition.

We perform some simulations under different values of diffusion coefficient κ ($\kappa = 0.05, 0.096, 0.15, 0.20, 0.25$) with the velocity $u = 1$ and different values of u ($u = 0.5, 0.8, 1.0, 1.2$) with the diffusion coefficient $\kappa = 0.08$, and plot the numerical and analytical results in Figs. 3 and 4 where $\Delta x = 1/40$ and $t = 6.0$. From these figures, one can observe that the numerical solutions of MRT-LB model and FLFD scheme are in good agreement with the analytical solutions. To show the convergence rates of the MRT-LB model and FLFD scheme for this problem, we also carry out some experiments under different values of lattice spacing changing from $\Delta x/8$ to $\Delta x = 1/10$, and the time step Δt is determined by a constant $\Delta^2 x/\Delta t$. We measure the RMSEs between the numerical and analytical solutions at the time $t = 6.0$ and show them in Figs. 5 and 6. As shown in these two figures, both the MRT-LB model and FLFD scheme have a fourth-order convergence rate in space, and the numerical results seem more accurate with the small u and proper κ. In addition, it is interesting that for these numerical experiments, the RMSEs and CRs of MRT-LB model and FDFL scheme are identical and are shown in Table I.

TABLE IV. The RMSEs and CRs of the MRT-LB model under different values of diffusion coefficient κ ($u = 1$).

u	κ	Δx	Δt	$\mathrm{RMSE}_{\Delta x,\Delta t}$	$\mathrm{RMSE}_{\Delta x/2,\Delta t/4}$	$\mathrm{RMSE}_{\Delta x/4,\Delta t/16}$	$\mathrm{RMSE}_{\Delta x/8,\Delta t/64}$	CR
1	0.050	1/10	1/25	3.9059×10^{-4}	7.1683×10^{-6}	3.2688×10^{-7}	1.8871×10^{-8}	∼4.7791
	0.060	1/10	1/50	2.8686×10^{-6}	1.7759×10^{-7}	1.3283×10^{-8}	8.6954×10^{-10}	∼3.8959
	0.080	1/10	1/50	7.8223×10^{-6}	3.6065×10^{-7}	2.0742×10^{-8}	1.2673×10^{-9}	∼4.1972
	0.096	1/10	1/50	6.6611×10^{-6}	3.0618×10^{-7}	1.7684×10^{-8}	1.0821×10^{-9}	∼4.1959
	0.120	1/10	1/50	3.5042×10^{-6}	1.4920×10^{-7}	8.5208×10^{-9}	5.2025×10^{-10}	∼4.2392
	0.150	1/10	1/200	9.8367×10^{-8}	6.2514×10^{-9}	3.9118×10^{-10}	2.4420×10^{-11}	∼3.9920
	0.200	1/10	1/200	3.1420×10^{-9}	1.9650×10^{-10}	1.2247×10^{-11}	7.6328×10^{-13}	∼4.0024
	0.250	1/10	1/100	1.2786×10^{-9}	7.2277×10^{-11}	4.3976×10^{-12}	2.7266×10^{-13}	∼4.0651

TABLE V. The RMSEs and CRs of the FLFD scheme under different values of diffusion coefficient κ ($u = 1$).

u	κ	Δx	Δt	$\mathrm{RMSE}_{\Delta x,\Delta t}$	$\mathrm{RMSE}_{\Delta x/2,\Delta t/4}$	$\mathrm{RMSE}_{\Delta x/4,\Delta t/16}$	$\mathrm{RMSE}_{\Delta x/8,\Delta t/64}$	CR
1	0.050	1/10	1/25	7.5642×10^{-5}	1.2665×10^{-6}	5.9709×10^{-8}	3.5019×10^{-9}	~4.7996
	0.060	1/10	1/50	4.6973×10^{-7}	3.4559×10^{-8}	2.6757×10^{-9}	1.7665×10^{-10}	~3.7922
	0.080	1/10	1/50	1.2667×10^{-6}	5.8362×10^{-8}	3.3767×10^{-9}	2.0726×10^{-10}	~4.1924
	0.096	1/10	1/50	1.0250×10^{-6}	4.8183×10^{-8}	2.8226×10^{-9}	1.7389×10^{-10}	~4.1750
	0.120	1/10	1/50	5.0085×10^{-7}	2.2243×10^{-8}	1.2986×10^{-9}	7.9995×10^{-11}	~4.2041
	0.150	1/10	1/200	1.3901×10^{-8}	8.9332×10^{-10}	5.6377×10^{-11}	3.5376×10^{-12}	~3.9800
	0.200	1/10	1/200	1.8638×10^{-9}	1.1883×10^{-10}	7.4868×10^{-12}	4.6960×10^{-13}	~3.9848
	0.250	1/10	1/50	1.4816×10^{-8}	8.6601×10^{-10}	5.3399×10^{-11}	3.3318×10^{-12}	~4.0395

Example 2. The second example we consider is a periodic problem

$$\begin{aligned} &\partial_t \phi + u\partial_x \phi = \kappa \partial_{xx}\phi, \quad (x,t) \in [-1,1] \times [0,\infty), \\ &\phi(x,0) = \sin(\pi x), \quad -1 \leqslant x \leqslant 1, \end{aligned} \tag{53}$$

with the periodic boundary condition adopted on boundaries of the computational domain $[-1, 1]$. Under the initial and periodic boundary conditions, we can derive the analytical solution to Eq. (53) [59],

$$\phi(x,t) = \sin[\pi(x-ut)]\exp(-\kappa\pi^2 t). \tag{54}$$

Similarly to the previous example, we first perform some simulations under different values of diffusion coefficient κ ($\kappa = 0.05, 0.06, 0.08, 0.12$) with $u = 1$ and different values of velocity u ($u = 0.05, 0.5, 1, 1.2$) with $\kappa = 0.1$. As shown in Figs. 7 and 8 where the lattice spacing $\Delta x = 1/20$, the numerical results are in good agreement with the analytical solutions at the time $t = 6.0$.

This problem is also applied to test the convergence rates of the MRT-LB model and FLFD scheme. For this purpose, we conduct a number of simulations with the specified parameters u and κ, and calculate the RMSEs under different lattice sizes. As seen from Figs. 9 and 10, Tables II, III, IV, and V where the simulations are suspended at the time $t = 6.0$ and the lattice spacing is varied from $\Delta x/8$ to $\Delta x = 1/10$ with a fixed $\Delta^2 x/\Delta t$, the present MRT-LB model and FLFD scheme have a fourth-order convergence rate in space, and also, the MRT-LB model and FLFD scheme are almost the same as each other.

VI. CONCLUSIONS

In this paper, we first developed an MRT-LB model for the one-dimensional CDE with a modefied equilibrium function f_i^{eq} through including an additional parameter $\eta = 2(1 - w_0)/w_0$, and then we performed the Chapman-Enskog analysis to recover the CDE (1) with the relation (13). Based on the MRT-LB model at the diffusive scaling, we also obtained an explicit FLFD scheme, which has a fourth-order accuracy in space once the weight coefficient w_0, the relaxation parameters s_1 and s_2 satisfy Eqs. (28a), (28b), and (28c). Through the detailed theoretical analysis, we derived the stability condition (31) of the MRT-LB model and FLFD scheme. Finally, we carried out some simulations, and the numerical results show that the MRT-LB model and FLFD scheme have fourth-order convergence rate in space, which is consistent with the accuracy analysis. It is worth mentioning that the MRT-LB model may be more efficient than FLFD scheme from a computational point of view since it is only a two-level method.

ACKNOWLEDGMENTS

The computation is completed in the HPC Platform of Huazhong University of Science and Technology. This work was financially supported by the National Natural Science Foundation of China (Grants No. 12072127 and No. 51836003).

APPENDIX: THE TWO SPECIAL CASES OF THE STABILITY ANALYSIS

Case 1. $s_2 = 1$. In this case, we can derive the following expressions from Eq. (32):

$$\Omega = 0, \quad A_{s_1} = A_{s_2} = 1, \tag{A1a}$$

$$\Omega_{s_1} = 0, \quad \Omega_{s_2} = 1 - s_1, \tag{A1b}$$

$$O_1 = (1 - s_1)[(w_0 - \sigma^2)(\omega - 1) + 1], \quad O_2 = 1, \tag{A1c}$$

$$C_{s_1} = 2 - s_1, \quad B = (2 - s_1)\omega - (w_0 - \sigma^2)(\omega - 1). \tag{A1d}$$

Then Eq. (31) can be simplified by

$$\max_{\omega\in[-1,1]} \left\{\sigma^2 s_1^2 (O_1+1)^2(1-\omega^2) + (O_1 - O_2)^2\left[B^2 - \left(O_1^2+1\right)^2\right]\right\} \leqslant 0. \tag{A2}$$

Substituting Eq. (A1) into Eq. (A2) yields

$$\max_{\omega\in[-1,1]} \left\{s_1^2\sigma^2(1-\omega^2)(1+O_1)^2 + (O_1-1)^2(B+O_1+1)(B-O_1-1)\right\} \leqslant 0, \tag{A3}$$

which can also be written as

$$\max_{\omega\in[-1,1]}\left\{s_1^2\sigma^2(1-\omega^2)(1+O_1)^2+(1-O_1)^2(1+O_1-B)[(1+O_1-B)-2(O_1+1)]\right\}\leqslant 0, \tag{A4}$$

or

$$\max_{\omega\in[-1,1]}\left\{s_1^2\sigma^2(1-\omega^2)(1+O_1)^2+(1-O_1)(1+O_1-B)\left[(1+O_1-B)(1-O_1)+2\left(O_1^2-1\right)\right]\right\}\leqslant 0. \tag{A5}$$

Multiplying $1/(1-\omega)$ on both sides of Eq. (A5) and with the help of $1+O_1-B=(2-s_1)(1-w_0+\sigma^2)(1-\omega)$, we have

$$\begin{aligned}\max_{\omega\in[-1,1]}&\left\{s_1^2\sigma^2(1+\omega)(1+O_1)^2+(2-s_1)(1-O_1)(1-w_0+\sigma^2)\right.\\&\left.\times\left[(2-s_1)(1-w_0+\sigma^2)(1-\omega)(1-O_1)+2\left(O_1^2-1\right)\right]\right\}\leqslant 0,\end{aligned} \tag{A6}$$

which is consistent with the result in Ref. [51].

Case 2. $u=0$. Under this condition, we have $\sigma=0$, and Eq. (31) becomes

$$\max_{\omega\in[-1,1]}\{(B^2-(O_1+O_2)^2)(O_1-O_2)^2\}\leqslant 0, \tag{A7}$$

or, equivalently,

$$\begin{aligned}\max_{\omega\in[-1,1]}&(-s_2(2-s_1)(1-\omega)(1-w_0)[1+(1-s_1)(1-s_2)]\\&\times\{s_2[w_0(\omega-1)+1][(s_2-1)(s_1-1)^2-1]-2[(s_2-1)^2(s_1-1)^2-1]\\&-\omega[(s_2-1)^2(s_1-1)+1](s_1-2)\\&+s_2[w_0(\omega-1)+1](s_2-2)(s_1-1)+s_1\omega(s_2-1)(s_1-2)\})\leqslant 0,\end{aligned} \tag{A8}$$

where $-s_2(2-s_1)(1-\omega)(1-w_0)[1+(1-s_1)(1-s_2)]\leqslant 0$ under the conditions of $0<s_1,s_2<2$, $0<w_0<1$ and $-1\leqslant\omega\leqslant 1$. After some manipulations, we can obtain

$$\begin{aligned}\max_{\omega\in[-1,1]}&(s_2(w_0(\omega-1)+1)\{[(s_2-1)(s_1-1)^2-1]+(s_2-2)(s_1-1)\}\\&-2[(s_2-1)^2(s_1-1)^2-1]+\omega(s_1-2)[(s_2-1)^2(1-s_1)-1+s_1(s_2-1)])\geqslant 0.\end{aligned} \tag{A9}$$

It is clear that the term on the right-hand side of Eq. (A9) is a linear function of ω, thus the maximum will be obtained at the point $\omega=-1$ or $\omega=1$ for any fixed s_1, s_2, and w_0,

$$\begin{aligned}\max\{&s_2(1-2w_0)[(s_2-1)(s_1-1)^2-1+(s_2-2)(s_1-1)]-2[(s_2-1)^2(s_1-1)^2-1]\\&-(s_1-2)[(s_2-1)^2(1-s_1)-1+s_1(s_2-1)],\\&s_2[(s_2-1)(s_1-1)^2-1+(s_2-2)(s_1-1)]-2[(s_2-1)^2(s_1-1)^2-1]\\&+(s_1-2)[(s_2-1)^2(1-s_1)-1+s_1(s_2-1)]\}\geqslant 0,\end{aligned}$$

which can be simplified by

$$\max\{2s_1s_2w_0[1-(1-s_1)(1-s_2)],\quad 2(2-s_2)(2-s_1)[1-(1-s_1)(1-s_2)]\}\geqslant 0. \tag{A10}$$

Actually, Eq. (A10) is an obvious result under $0<s_1,s_2<2$ and $0<w_0<1$. This also means that the MRT-LB model and FLFD scheme are unconditionally stable, which are consistent with the available work [8].

[1] S. Chen and G. Doolen, Lattice Boltzmann method for fluid flows, Annu. Rev. Fluid Mech. **30**, 329 (1998).

[2] S. Succi, *The Lattice Boltzmann Equation for Fluid Dynamics and Beyond* (Oxford University Press, Oxford, 2001).

[3] C. K. Aidun and J. R. Clausen, Lattice-Boltzmann method for complex flows, Annu. Rev. Fluid Mech. **42**, 439 (2010).

[4] Z. Guo and C. Shu, *Lattice Boltzmann Method and Its Applications in Engineering* (World Scientific Publishing, Singapore, 2013).

[5] T. Krüger, H. Kusumaatmaja, A. Kuzmin, O. Shardt, G. Silva, and E. M. Viggen, *The Lattice Boltzmann Method: Principles and Practice* (Springer, Switzerland, 2017).

[6] H. Wang, X. Yuan, H. Liang, Z. Chai, and B. Shi, A brief review of the phase-field-based lattice Boltzmann method for multiphase flows, Capillarity **2**, 33 (2019).

[7] C. Huber, B. Chopard, and M. Manga, A lattice Boltzmann model for coupled diffusion, J. Comput. Phys. **229**, 7956 (2010).

[8] Y. Lin, N. Hong, B. Shi, and Z. Chai, Multiple-relaxation-time lattice Boltzmann model-based four-level finite-difference scheme for one-dimensional diffusion equations, Phys. Rev. E **104**, 015312 (2021).
[9] S. Suga, An accurate multi-level finite difference scheme for 1D diffusion equations derived from the lattice Boltzmann method, J. Stat. Phys. **140**, 494 (2010).
[10] R. Straka and K. V. Sharma, An accuracy analysis of the cascaded lattice Boltzmann method for the 1D advection-diffusion equation, Comput. Methods Mater. Sci. **20**, 174 (2020).
[11] R. G. M. van der Sman and M. H. Ernst, Convection-diffusion lattice Boltzmann scheme for irregular lattices, J. Comput. Phys. **160**, 766 (2000).
[12] I. Ginzburg, Equilibrium-type and link-type lattice Boltzmann models for generic advection and anisotropic-dispersion equation, Adv. Water Resour. **28**, 1171 (2005).
[13] I. Rasin, S. Succi, and W. Miller, A multi-relaxation lattice kinetic method for passive scalar diffusion, J. Comput. Phys. **206**, 453 (2005).
[14] B. Shi and Z. Guo, Lattice Boltzmann model for nonlinear convection-diffusion equations, Phys. Rev. E **79**, 016701 (2009).
[15] B. Chopard, J. L. Falcone, and J. Latt, The lattice Boltzmann advection-diffusion model revisited, Eur. Phys. J.: Spec. Top. **171**, 245 (2009).
[16] H. Yoshida and M. Nagaoka, Multiple-relaxation-time lattice Boltzmann model for the convection and anisotropic diffusion equation, J. Comput. Phys. **229**, 7774 (2010).
[17] I. Ginzburg, Multiple anisotropic collisions for advection-diffusion lattice Boltzmann schemes, Adv. Water Resour. **51**, 381 (2013).
[18] Z. Chai and T. S. Zhao, Lattice Boltzmann model for the convection-diffusion equation, Phys. Rev. E **87**, 063309 (2013).
[19] Z. Chai, B. Shi, and Z. Guo, A multiple-relaxation-time lattice Boltzmann model for general nonlinear anisotropic convection-diffusion equations, J. Sci. Comput. **69**, 355 (2016).
[20] O. Aursjø, E. Jettestuen, J. L. Vinningland, and A. Hiorth, An improved lattice Boltzmann method for simulating advective-difusive processes in fluids, J. Comput. Phys. **332**, 363 (2017).
[21] L. Li, Multiple-time-scaling lattice Boltzmann method for the convection-diffusion equation, Phys. Rev. E **99**, 063301 (2019).
[22] J. Michelet, M. M. Tekitek, and M. Berthier, Multiple relaxation time lattice Boltzmann schemes for advection-diffusion equations with application to radar image processing, J. Comput. Phys. **471**, 111612 (2022).
[23] M. Hirabayashi, Y. Chen, and H. Ohashi, The lattice BGK model for the Poisson equation, JSME Int. J. Ser. B **44**, 45 (2001).
[24] Z. Chai and B. Shi, A novel lattice Boltzmann model for the Poisson equation, Appl. Math. Model. **32**, 2050 (2008).
[25] Z. Chai, H. Liang, R. Du, and B. Shi, A lattice Boltzmann model for two-phase flow in porous media, SIAM J. Sci. Comput. **41**, B746 (2019).
[26] Q. Li, Z. Zheng, S. Wang, and J. Liu, A multilevel finite difference scheme for one-dimensional Burgers equation derived from the lattice Boltzmann Method, J. Appl. Math. **2012**, 925920 (2012).
[27] L. Zhong, S. Feng, P. Dong, and S. Gao, Lattice Boltzmann schemes for the nonlinear Schrödinger equation, Phys. Rev. E **74**, 036704 (2006).
[28] S. Succi, Lattice Boltzmann method for quantum field theory, J. Phys. A: Math. Theor. **40**, F559 (2007).
[29] S. Palpacelli and S. Succi, Numerical validation of the quantum lattice Boltzmann scheme in two and three dimensions, Phys. Rev. E **75**, 066704 (2007).
[30] B. Shi and Z. Guo, Lattice Boltzmann model for the one-dimensional nonlinear Dirac equation, Phys. Rev. E **79**, 066704 (2009).
[31] Y. H. Qian, D. d'Humière, and P. Lallemand, Lattice BGK models for Navier-Stokes equation, Europhys. Lett. **17**, 479 (1992).
[32] Z. Chai and B. Shi, Multiple-relaxation-time lattice Boltzmann method for the Navier-Stokes and nonlinear convection-diffusion equations: Modeling, analysis, and elements, Phys. Rev. E **102**, 023306 (2020).
[33] Z. Chai and T. S. Zhao, Nonequilibrium scheme for computing the flux of the convection-diffusion equation in the framework of the lattice Boltzmann method, Phys. Rev. E **90**, 013305 (2014).
[34] P. Lallemand and L. S. Luo, Theory of the lattice Boltzmann method: dispersion, dissipation, isotropy, Galilean invariance, and stability, Phys. Rev. E **61**, 6546 (2000).
[35] C. Pan, L.-S. Luo, and C. T. Miller, An evaluation of lattice Boltzbmann schemes for porous medium flow simulation, Comput. Fluids **35**, 898 (2006).
[36] S. Cui, N. Hong, B. Shi, and Z. Chai, Discrete effect on the halfway bounce-back boundary condition of multiple-relaxation-time lattice Boltzmann model for convection-diffusion equations, Phys. Rev. E **93**, 043311 (2016).
[37] L.-S. Luo, W. Liao, X. Chen, Y. Peng, and W. Zhang, Numerics of the lattice Boltzmann method: Effects of collision models on the lattice Boltzmann simulations, Phys. Rev. E **83**, 056710 (2011).
[38] S. Chapman and T. G. Cowling, *The Mathematical Theory of Nonuniform Gases* (Cambridge University Press, Cambridge, UK, 1970).
[39] E. Ikenberry and C. Truesdell, On the pressures and the flux of energy in a gas according to Maxwell's kinetic theory, I, J. Ration. Mech. Anal. **5**, 1 (1956).
[40] W.-A. Yong, W. Zhao, and L.-S. Luo, Theory of the lattice Boltzmann method: Derivation of macroscopic equations via the "Maxwell" iteration, Phys. Rev. E **93**, 033310 (2016).
[41] D. J. Holdych, D. R. Noble, J. G. Georgiadis, and R. O. Buckius, Truncation error analysis of lattice Boltzmann methods, J. Comput. Phys. **193**, 595 (2004).
[42] A. Wagner, Thermodynamic consistency of liquid-gas lattice Boltzmann simulations, Phys. Rev. E **74**, 056703 (2006).
[43] F. Dubois, Equivalent partial differential equations of a lattice Boltzmann scheme, Comput. Math. Appl. **55**, 1441 (2008).
[44] F. Dubois, Third order equivalent equation of lattice Boltzmann scheme, Discr. Contin. Dyn. Syst. **23**, 221 (2009).
[45] F. Dubois, Nonlinear fourth order Taylor expansion of lattice Boltzmann schemes, Asympt. Analy. **127**, 297 (2022).
[46] M. Junk, A finite difference interpretation of the lattice Boltzmann method, Numer. Methods Part. Diff. Equ. **17**, 383 (2001).
[47] P. V. Coveney, A lattice kinetic scheme for incompressible viscous flows with heat transfer, Philos. Trans. R. Soc. A **360**, 477 (2002).

[48] M. G. Ancona, Fully-lagrangian and lattice-boltzmann methods for solving systems of conservation equations, J. Comput. Phys. **115**, 107 (1994).

[49] E. C. Du Fort and S. P. Frankel, Stability conditions in the numerical treatment of parabolic differential equations, Math. Comput. **7**, 135 (1953).

[50] S. Dellacherie, Construction and analysis of lattice Boltzmann methods applied to a 1D convection-Diffusion equation, Acta. Appl. Math. **131**, 69 (2014).

[51] T. Bellotti, B. Graille, and M. Massot, Finite Difference formulation of any lattice Boltzmann scheme, Numer. Math. **152**, 1 (2022).

[52] T. Bellotti, Rigorous derivation of the macroscopic equations for the lattice Boltzmann method via the corresponding Finite Difference scheme, arXiv:2205.02505v1.

[53] D. d′Humière and I. Ginzburg, Viscosity independent numerical errors for lattice Boltzmann models: From recurrence equations to "magic" collision numbers, Comput. Math. Appl. **58**, 823 (2009).

[54] I. Ginzburg, Truncation errors, exact and heuristic stability analysis of two-relaxation-times lattice Boltzmann schemes for anisotropic advection-diffusion equation, Commun. Comput. Phys. **11**, 1439 (2012).

[55] Z. Chai, C. Huang, B. Shi, and Z. Guo, A comparative study on the lattice Boltzmann models for predicting effective diffusivity of porous media, Int. J. Heat Mass Transf. **98**, 687 (2016).

[56] Y. Qian and Y. Zhou, Higher-order dynamics in lattice-based models using the Chapman-Enskog method, Phys. Rev. E **61**, 2103 (2000).

[57] I. Ginzburg, D. d′Humière, and A. Kuzmin, Optimal stability of advection-diffusion lattice Boltzmann models with two relaxation times for positive/negative equilibrium, J. Stat. Phys. **139**, 1090 (2010).

[58] A. Kuzmin, I. Ginzburg, and A. A. Mohamad, The role of the kinetic parameter in the stability of two-relaxation-time advection-diffusion lattice Boltzmann schemes, Comput. Math. Appl. **61**, 3417 (2011).

[59] A. Mojtabi and M. O. Deville, One-dimensional linear advection-diffusion equation: Analytical and finite element solutions, Comput. Fluids **107**, 189 (2015).